Assessing the Effectiveness of 3D-Printed Ceramic Structures for Coral Restoration: Growth, Survivorship, and Biodiversity Using Visual Surveys and eDNA

Authors: Vriko Yu[1†], Alison Corley[1†], Shelby McIlroy[2], Jane Wong[1], Zhongyue Wilson Wan[1], Horace Lau[1], David M. Baker[*1]

[†] Vriko Yu and Alison Corley should be considered joint first author

*Corresponding author: David M. Baker, School of Biological Sciences, The University of Hong Kong, Kadoorie Biological Sciences Building 6S-14, Pokfulam Road,
Lung Fu Shan, Hong Kong, P.R. China. Email: dmbaker@hku.hk

Affiliations:
[1]School of Biological Sciences, The Swire Institute of Marine Science, The University of Hong Kong, Hong Kong, P.R. China
[2]Simon F.S. Li Marine Science Laboratory, School of Life Sciences, The Chinese University of Hong Kong, Hong Kong, P.R. China

Key Words: Coral restoration, artificial reefs, environmental DNA (eDNA), ecosystem monitoring, coral reefs, coral transplantation.

Abstract

With coral reefs undergoing widespread degradation, various artificial structures have been developed to mitigate losses in coral cover. These structures primarily serve as substrates for coral transplantation, with the expectation that growing corals will attract and provide habitat for reef-associated taxa. However, designs for these structures commonly neglect the substrate's ability to directly support the diverse array of small and encrusting organisms that comprise a coral reef ecosystem. In a pilot deployment in Hong Kong, we tested a novel 3D-printed structure — modular tiles made of porous terra cotta with complex surface structures intended to enhance micro- and cryptic biodiversity — for coral reef restoration. Over four years, we monitored the condition and growth of 378

outplanted coral fragments through diver assessments and photogrammetric measurements. Changes in biodiversity were evaluated using visual surveys and eDNA metabarcoding. We recorded high survivorship, with 91% of transplanted corals alive and securely attached at end of the monitoring period. Greater fish and macroinvertebrate abundance were observed at the restoration site than at a nearby unrestored area. eDNA analyses indicated a 23.5% increase in eukaryote ASV richness at the restoration site relative to the unrestored site, and a 13.3% increase compared to a natural reference coral community. As the first example of eDNA being used to detect changes in eukaryote diversity associated with coral reef restoration, this study demonstrates the tiles' dual function: (1) sustaining coral growth and (2) enhancing cryptic reef biodiversity, an outcome often overlooked in conventional reef restoration design and monitoring.

Introduction

Coral reefs are declining at an alarming rate. Driven by the combined impacts of climate change, overfishing, eutrophication, and coastal development, coral cover worldwide has already declined by over 50% since the late 20th century, with some regions — such as the Caribbean — experiencing losses of more than 80% (Gardner et al., 2003; Bruno and Valdivia, 2016; Hochberg and Gierach, 2021; Whaley et al., 2023). As mass bleaching events and coral mortality become more frequent and intense, over 90% of the world's reefs are projected to face severe degradation by the middle of the century (Grottoli et al., 2014; Kalmus et al., 2022). This collapse threatens not only marine biodiversity — with up to a quarter of all marine species depending on coral reefs (Reaka, 1997; Knowlton et al., 2010; Cowen and Putnam, 2022) — but also the livelihoods of roughly 500 million people and ecosystem services valued at up to USD 350,000 per hectare annually (Battaglia, 2023; Edwards et al., 2024).

In response, Artificial Reefs (ARs) have emerged as one of the most widely used interventions to stabilize degraded reef structures, promote coral settlement, and support broader ecological recovery (Boström-Einarsson et al., 2020; Higgins et al., 2022). ARs range from simple rubble piles and concrete blocks to complex, biomimetic structures designed to increase surface area, reduce hydrodynamic stress, and provide microhabitats for diverse marine organisms (Sedano et al., 2020). When combined with coral outplanting, ARs can enhance survivorship and potentially accelerate the recovery of benthic communities. However, many ARs remain reliant on non-biocompatible materials, provide minimal fine-scale habitat complexity, are unsuited for sediment-laden or high-energy environments, and are limited in their scalability for covering large areas. In addition, few artificial structures produced for coral reef restoration explicitly consider cryptic biodiversity or long-term ecological function in their design, with most focusing solely on mitigating losses in coral cover (Higgins et al., 2022).

To address these limitations, we developed a ceramic 3D-printed reef tile, engineered from terracotta clay and designed to integrate both coral restoration and

biodiversity enhancement through a scalable, modular design. The tiles feature a hexagonal configuration and fine-scale topography intended to promote coral attachment, reduce sediment smothering, and replicate natural reef crevices, thus facilitating larval recruitment and benthic colonization (Hata et al., 2017; Levy et al., 2022). Unlike conventional concrete ARs or floating nurseries, the reef tiles are deployable directly onto soft benthic substrates without complex substrate engineering, offering a low-impact solution for challenging or urbanized environments. The material properties of terracotta — being porous, erosion-resistant, and biocompatible — further support microbial colonization and ecological succession, enhancing both coral health and overall habitat function (Spieler et al., 2001; Vivier et al., 2021). Yet, the effectiveness of these design choices requires empirical validation. Beyond coral fragment survivorship, the potential of the artificial structures and the outplanted coral community to facilitate the reassembly of reef-associated taxa — which are critical for restoring ecological function — must also be assessed under dynamic, real-world conditions.

While coral survivorship remains a central restoration target, ecosystem resilience depends equally on the reassembly of diverse coral-associated communities that sustain trophic interactions and contribute to reef function (Done, 1992; Wismer et al., 2009; Edwards et al., 2010; Boström-Einarsson et al., 2020). Owing to their relative ease of identification, sensitivity to environmental disturbance, and role in mitigating macroalgal overgrowth, macroinvertebrates and fish are often the only targets for biodiversity monitoring in coral restoration projects (Hein et al., 2017). Beyond these two taxonomic groups however, are a range of organisms that provide equally critical functions on coral reefs: Crustose coralline algae provide larval settlement cues, sponges consolidate loose sediments and rubble, smaller cryptic invertebrates also feed on algae and act as a food source for reef fish — while all of these examples, in combination with the microbial communities of bacteria, algae, and fungi, facilitate nutrient cycling (Bourne et al., 2016).

To capture a fuller picture of the effect of the artificial reef tiles on community diversity, we combined standard SCUBA-based visual surveys of fish and macroinvertebrates with environmental DNA (eDNA) metabarcoding, a non-invasive tool

that enables detection of both conspicuous and cryptic taxa from environmental samples (Leray and Knowlton, 2015; Beng and Corlett, 2020). eDNA is a particularly useful tool for monitoring structurally complex systems like coral reefs, where its ability to detect a wide range of organisms complements traditional visual surveys and bridges critical gaps in current restoration monitoring frameworks (Thompson et al., 2024). In this study, we evaluated the ecological performance of 3D-printed ceramic reef tiles deployed in a subtropical, urbanized marine environment to determine whether this engineered substrate can support scalable coral restoration while promoting broader biodiversity uplift with the goal of providing a replicable model for effective, ecosystem-based reef rehabilitation.

Materials and Methods

Study Sites

Despite lying just north of the Tropic of Cancer, Hong Kong supports a surprising level of coral diversity, with more than 90 species of reef-building corals recorded across its semi-enclosed, estuarine-influenced waters (Duprey et al., 2017) This diversity is particularly noteworthy, given the region's marked seasonal variability and persistent anthropogenic stressors, such as coastal development, salinity fluctuations, and sediment-laden runoff (Fabricius, 2005; Xie et al., 2020). Coral cover in Hong Kong declined substantially over the past century, driven by acute stressors such as thermal anomalies and extreme weather events, alongside chronic local pressures like nutrient enrichment and elevated suspended solids (Cybulski et al., 2020, Yeung et al., 2021). Since the 1990s, however, water quality in Hong Kong has improved due to stricter controls on wastewater treatment (Hua et al., 2008). Hong Kong thus presents a suitable environment to explore the viability of re-introducing extirpated corals following a reduction in the extent of local environmental stressors (Duprey et al., 2017).

This study was conducted within Hoi Ha Wan Marine Park (HHWMP; 22°28'13.68"N, 114°20'08.25"E), located in the northeastern waters of the Sai Kung Peninsula, Hong Kong SAR (Figure 1). Established in 1996, HHWMP spans approximately 260 hectares and is known for its diverse subtropical coral communities, supporting more than 60 species of hard corals (AFCD Report, 2004). The park experiences pronounced seasonal variation, with sea surface temperatures ranging from 15 °C in winter to 28 °C in summer, and salinity modulated by monsoonal rainfall and freshwater inflow. These dynamic conditions, combined with proximity to urbanized coastal zones, positions HHWMP as a representative site for testing coral restoration strategies in marginal, subtropical reef environments.

Three ecologically distinct sites within HHWMP were selected for comparative analysis (Figure 1). The Restored site, off Coral Beach, served as the primary deployment area for the reef tiles. Prior to the installation of the artificial structures, this site was a

sandy seabed with no coral cover or hard substrate. Approximately 50 m north of the restored area, parallel to the shoreline, the Unrestored site comprised a section of sandy seabed with no artificial substrate, representing a degraded benthic baseline with no intervention. The Reference site, situated at Gruff Head approximately 500 m west of the restored site, featured a natural coral assemblage and minimal anthropogenic disturbance. This site was selected to represent a realistic restoration target for community diversity and function. All three sites were located at comparable depths (6-8 m) and experienced similar hydrodynamic and environmental conditions.

Reef Tile Design

The 3D-printed ceramic reef tiles used in this study were custom-engineered ceramic substrates designed to promote coral recruitment, enhance structural complexity, and mitigate sediment accumulation in a subtropical marine environment. Each tile was hexagonal in shape, with a maximum width of 650 mm, and comprised two integrated functional layers: a structural base layer ("grid layer") and a biomimetic surface layer ("coral layer") (Figure 2). The grid layer featured a diagrid framework with integrated lateral bracing to maximize mechanical stability while minimizing material usage and fabrication defects. The geometry was optimized to reduce cracking during drying and thermal stress during firing, with a print path totaling approximately 170 m in length. This design facilitated uniform moisture evaporation and enhanced compressive strength under load. To improve hydrodynamic performance and minimize sediment deposition, a three-legged footing system was printed on the underside of each tile after drying (Figure 2). These legs elevated the tile slightly above the seabed to promote water flow and create a sheltered interface for benthic recruitment.

Fabrication of the 3D-printed Reef tiles was performed using a Direct Ink Writing (DIW) method with an ABB 6700 robotic arm and a Deltabots linear ram extruder (6 mm nozzle diameter). The paste material consisted of red terracotta clay (P1331, Potterycrafts Ltd, UK) amended with <1% fine crystalline silica. Tiles were printed with a layer height of 2.7 mm at extrusion speeds ranging from 10.5 to 17 mm/s depending on local path

geometry. After air-drying and structural inspection, tiles were fired in a gas kiln at 1125 °C, yielding a mean shrinkage of approximately 11%.

Restoration Site Design

The coral restoration experiment was conducted within a 10 m × 35 m plot at the Restored site (Coral Beach) in Hoi Ha Wan Marine Park (Figure 3). Within this plot, a total of 24 modular reef units — comprising 72 reef tiles — were deployed in a grid layout with 5 m spacing between units. Each unit consisted of three interlocked tiles arranged in a triangular configuration (Figure 2). This modular design enhanced structural heterogeneity while facilitating standardized monitoring across units.

Each reef tile was seeded with six evenly spaced coral fragments, representing three distinct morpho-functional groups: *Acropora* (branching), *Pavona* (plating), and *Platygyra* (massive). *Pavona* and *Platygyra* fragments were collected as Corals of Opportunity within HHWMP, while *Acropora* fragments were sourced from healthy donor colonies at Bluff Island (~8 km distance from the restoration site), due to their local extirpation within the marine park. A total of 378 fragments were transplanted to the restoration site, consisting of 126 fragments per genus. Coral fragments were secured using marine-grade epoxy (Z-Spar A-788).

Monitoring Coral Survivorship and Growth

Coral performance was assessed quarterly for four years following transplantation, beginning three months after outplanting. SCUBA divers visually examined each coral fragment for signs of bleaching or discoloration at each survey interval. Five conditions were assigned to the coral fragments: healthy, partial mortality, detached, dead, and broken. During each monitoring event, high-resolution photographs of each tile and its attached coral fragments were captured using an underwater digital camera (Olympus TG5). Each image included a scale bar placed on the tile, which served as a calibration reference for accurate spatial measurements. Growth measurements were extracted from

these photographs using ImageJ software (version 1.52n), recording the maximum linear extension of each coral fragment at each survey date.

Extension rates (linear growth in cm month^{-1}) for each coral individual were calculated based on the change in size from the initial measurement to the monitoring survey (*i* = 1-14):

$$Extension\ rate_i = \frac{Size_i - Size_{initial}}{Time_i}$$

where $Size_i$ represents the size at the monitoring survey, $Size_{initial}$ is the initial size measurement, and $Time_i$ is the time interval (in month) since the initial measurement.

Differences in growth rates between genera were tested for with GLMMs (*glmmTMB* package; Brooks et al. 2017). The model included fixed effects for genus, with random factor specified for coral fragments nested within transplantation tiles, which were themselves nested within units to capture variability at multiple hierarchical levels. To address temporal autocorrelation among repeated measures on the same coral fragment, a first-order autoregressive (AR1) variance structure was incorporated. Pairwise comparisons of estimated marginal means were performed using the emmeans package (Lenth et al. 2024), when significant difference between genera was detected, with Kenward-Roger degrees-of-freedom method and Tukey-adjusted *p*-values.

Visual Fish and Invertebrate Surveys

To assess reef community's response to restoration, visual belt transect surveys were conducted concurrently with coral monitoring at all three study sites. At each site, three 35-meter transects were laid out parallel to the shoreline, spaced 5 m apart. Two divers surveyed each transect simultaneously (one on each side), covering a total area of 2 × 35 m per transect. Target species (Table 1) were selected from the list of Reef Check bioindicator species for Hong Kong, which identifies common fish and invertebrate that are used to represent key functional groups and responses to different anthropogenic stressors acting on subtropical reef ecosystems (Indo-Pacific: Hodgson et al. 2006; Hong Kong: AFCD). The monitored species included herbivores, predators, and ecosystem engineers, all of which serve as indicators of reef health.

Environmental DNA Metabarcoding

DNA Sampling, Extraction, Amplification, and Sequencing

Two years after the artificial tile deployment, sedimentary environmental DNA (eDNA) was sampled from all three study sites. Five replicates were collected at 5-6 m depth from each site, with 10 m distance between each replicate. Each replicate was collected in a sterile 50 mL falcon tube, collecting only sediment from the top 1 cm of the seafloor. Samples were transported back to the laboratory on ice and stored at -20 °C within three hours of collection. Each sample was homogenized using a sterile spatula and plastic tray, and a 500 mg aliquot of bulk sediment weighed for extraction. DNA was extracted using the DNeasy PowerMax Soil Kit following the manufacturer's protocol and subsequently purified using the DNeasy PowerClean Cleanup Kit (Qiagen). The concentration of the resulting DNA extracts was quantified using the Qubit dsDNA High Sensitivity Assay (Thermo Fisher Scientific).

Extracted DNA was amplified using the mlCOIintF and jgHCO2198 primer set, which amplifies a ~313bp fragment of the cytochrome c oxidase subunit I (COI) gene to target metazoan diversity. Polymerase chain reactions (PCR) were prepared to a 20 uL total reaction volume. The reaction mixture included 2 µL of 10X Advantage 2 PCR Buffer (Takara Bio), 0.4 µL of 50X Advantage 2 Polymerase Mix, 1.4 µL of a 50X dNTP Mix (10 mM each), 1 µL of each primer (10 pmol/µL), 0.5 µL Bovine Serum Albumin (20 mg/mL), and 10 to 30 ng of template DNA. The following thermocycling parameters were used: an initial 1 minute at 95 °C, followed by 16 cycles of denaturing at 95 °C for 10 seconds, annealing at 62 °C for 30 seconds, and extension at 72 °C for 1 minute, ending with 10 minutes of final extension at 72 °C. To increase the probability of amplification for low-copy DNA sequences, DNA extracted from each sample was amplified in triplicate. At minimum, one PCR control was performed per seven sample reactions using autoclaved MQ as the template. PCR products were visualised via electrophoresis in a 2% agarose gel. Triplicate amplification products for each sample were then pooled and subsequently purified using the QIAquick Gel Extraction Kit (Qiagen). A unique 6 bp indexing primer was attached to each pooled sample.

Library preparation and sequencing was completed by Genewhiz (Suzhou, China). All 15 samples submitted for sequencing passed initial quality control, with DNA concentrations ranging between 0.2 and 23.4 ng/μL. Sequencing was performed on an Illumina MiSeq system. A total of 24.6 million 251 bp paired-end reads were generated, with 1.4 to 1.8 million reads per sample. A binned quality score of Q30 (indicating base-call accuracy of 99.9%) was given to 90% of base calls.

Bioinformatics

Sequence Analysis and Quality Control

Raw sequencing reads were processed in *QIIME2* (v2022.2; Boylen et al., 2019) using the *DADA2* plugin (v1.22; Callahan et al., 2016). Reads were demultiplexed in *QIIME2*. The *denoise-paired* function of *DADA2* was used to trim primers, denoise and join paired reads, dereplicate duplicate sequences, and remove chimeric sequences. Forward and reverse reads were both trimmed by 26 bp at the 5' end and truncated at the 3' end at 250 bp. Chimeras were removed based on the consensus method. A total of 117,673 amplicon sequence variants (ASVs), represented by 18,704,812 reads, were inferred. Taxonomy was then assigned using the Ribosomal Database Program (*RDP*) classifier v2.13 (Wang et al., 2007), with a pre-trained database of *COI* reference sequences (v4; Porter, 2017; Porter and Hajibabaei, 2018). Taxonomic nomenclature was manually edited as needed to adhere to the terminology established by the World Register of Marine Species (*WoRMS*; www.marinespecies.org).

Following taxonomic assignment, data were imported into *R* (v4.2.1; R Core Team, 2018) for further filtering and analysis using the *phyloseq* package (v1.38; McMurdie and Holmes, 2013). Alpha rarefaction curves were plotted using the *ggrare()* function of the *ranacapa* package (v0.1; Kandlikar et al., 2018). One sample from the unrestored site had anomalously low ASV richness (974 ASVs) relative to other samples from the same site (4,813 to 16,559 ASVs per sample; Figure 2), with the overwhelming majority of reads from this sample (>95.6%) assigned to only two species. This sample did not meet quality standards and was removed from the dataset.

Singletons (1,050 ASVs) were then removed, and sequences assigned to Bacteria (23,568 ASVs), Archaea (3 ASVs), or terrestrial taxa (6,431 ASVs) were discarded.

Stringent prevalence and abundance filters were applied to eliminate spurious ASVs produced by background sequencing errors during apparent over-sequencing (Figure S1). Only ASVs that appeared in at least three samples from each site were retained. To mitigate bias in prevalence filtering introduced by unequal replication between sites, a mock sample was generated by randomly sampling from a combined pool of ASVs from all other unrestored site samples (seed value = 852). The prevalence filter removed 94.8% of the remaining ASVs (81,583 ASVs), which accounted for 41.8% of the remaining sequencing reads. ASVs were then filtered based on abundance, removing those with a cumulative read abundance of fewer than 50 total counts across all samples (493 ASVs). Samples were then rarefied to an even sequencing depth (96,443 reads per sample, 90% of the depth of the sample with the lowest number of reads; Figure S1). No ASVs were removed through rarefaction.

Community Diversity Analysis

All analyses were performed in *R* using *phyloseq* (v1.38; McMurdie and Holmes, 2013). Figures were created using *ggplot2* (v3.5.2; Wickham, 2016). A tandem approach was adopted to examine taxonomic composition and differences in community structure between sites, using both occurrence and relative read abundance data. Two transformed ASV tables were utilized: one in which read counts were converted to a binary presence-absence matrix, and another in which read counts were retained and normalized through Hellinger transformation. For metrics and visualizations based on the site-level eDNA community, ASV counts for each replicate were merged by site prior to transformation.

Observed ASV richness was used to measure alpha diversity, comparing both the number of unique ASVs detected across all samples for each site and the ASV richness of each replicate by site. To test whether there was a significant difference in sample ASV richness between sites, a one-way analysis of variance (ANOVA) was conducted with the *vegan* package (v2.5; Okansen et al., 2020). Homogeneity of variance and normality were verified by Levene's and Shapiro's tests using the *rstatix* package (v0.7; Kassambara,

2021). The ASV richness of the 10 most diverse phyla by site was visualized as a stacked bar plot, with the number of ASVs among the remaining, less-represented phyla pooled into one group. A chi-squared contingency table test was used to determine whether ASV richness for individual phyla varied significantly by site, using the *chisq.test()* function of the *stats* package. To minimize statistical bias introduced by uneven ASV richness across different phyla, only phyla represented by at least 50 ASVs were included in the chi-squared test, and two versions of the test were conducted: one including Bacillariophyta, which had a significantly higher number of ASVs compared to all other taxa, and another excluding Bacillariophyta.

Beta diversity was assessed using two dissimilarity matrices: one based on the Jaccard index, calculated from occurrence data only, and another based on Bray-Curtis dissimilarity, calculated from Hellinger-transformed read abundances. Principal coordinate ordinations (PCoA) based on each of these matrices were produced to visualize differences in community composition between samples. Differences between sites were then tested using permutational analyses of variance (PERMANOVA) on both matrices with the *adonis2* function of *vegan*. This was followed by post-hoc pairwise comparisons using the *pairwiseAdonis* wrapper for *vegan* (Martinez Arbizu, 2020). Taxonomic composition plots were created from the Hellinger-transformed read count matrix. Three plots were generated: (1) total Hellinger-transformed read abundance by sample, to better understand variation in sample composition among replicates from the same site; (2) compositional abundance by site, where sample data were merged, Hellinger-transformed, and then converted to relative abundance data to approximate a consensus composition for each site; and (3) another version of the same site-level compositional abundance, but with Bacillariophyta sequences removed prior to data transformation, to better examine differences in the relative abundance of less-abundant phyla.

Results

Coral Performance

Coral Transplant Growth and Survival

Survivorship of transplanted coral fragments remained high throughout the four-year monitoring period, with 91% of individuals (n = 378) classified as alive and securely attached at the study's conclusion (Figure 4; Table S1). Overall, 90% of all coral fragments were alive, and only 2% exhibited signs of partial tissue loss. Full mortality occurred in just 2% of fragments, while 8% were lost due to detachment from the reef tile (Table S1). Mortality and detachment rates remained low and stable over time, indicating sustained substrate stability and fragment viability at the restoration site. No bleaching events were recorded during the monitoring surveys.

Genus-level analysis revealed variation in resilience among the three coral growth morphologies (Figure 4). *Acropora* exhibited the highest survivorship, with 95% of fragments remaining healthy and only 1% showing partial tissue loss. *Platygyra* demonstrated moderately reduced performance, with 89% of fragments healthy, 5% exhibiting partial mortality, and 3% dead. In contrast, *Pavona* showed the lowest survivorship, with only 79% classified as healthy and 3% dead.

Tukey's pairwise comparisons (Table 2) indicated that *Acropora* had a significantly higher survival rate than *Platygyra* ($z = -2.535$, $p < 0.05$) and *Pavona* ($z = -9.891$, $p < 0.001$), while *Platygyra* also exhibited significantly greater survivorship compared to *Pavona* ($z = 9.132$, $p < 0.001$). Conversely, the incidence of broken fragments was highest in *Acropora* (61%), significantly exceeding that of *Platygyra* (5%, $p < 0.001$) and *Pavona* (10%, $p < 0.001$). Additionally, *Platygyra* had a significantly higher breakage rate than *Pavona* ($p < 0.005$). Furthermore, *Pavona* exhibited a significantly higher detachment rate at 17%, compared to 4% in *Acropora* ($p < 0.001$) and 3% in *Platygyra* ($p < 0.001$).

Extension Rates

Over the four-year monitoring period, all three coral genera exhibited positive linear extension relative to their initial transplantation size, though significant differences in growth trajectories were observed among genera representing distinct growth forms (Figure 5). *Acropora* fragments showed the most pronounced increase in linear extension, with a mean growth of 260% relative to baseline measurements, corresponding to an extension rate of 0.35 ± 0.16 cm month-1 (n = 1178). *Pavona* displayed intermediate growth, achieving a mean increase of 169%, with an extension rate of 0.21 ± 0.11 cm month-1 (n = 996). In contrast, *Platygyra*, characterized by its massive growth form and inherently slower growth dynamics, with a mean increase of 108% and an extension rate of 0.15 ± 0.07 cm month-1 (n = 978). Tukey-adjusted contrasts of growth rates (Table 2) showed that *Acropora* grew significantly faster than *Pavona* (z = 8.437, $p < 0.001$) and *Platygyra* (z = 14.324, $p < 0.001$). *Pavona* also grew faster than *Platygyra* (z = 5.752, $p < 0.001$).

Bioindicator Surveys

The total abundance of fish (Figure 6; Table 3) differed significantly among the sites (Table 4; Kruskal-Wallis $\chi^2(2) = 54.1$, $p < 0.001$, $\eta^2 = 0.104$). Post-hoc pairwise comparisons showed that the average fish abundance at the unrestored site (0.2 ± 0.6) was significantly lower than both the reference (1.2 ± 1.8; $p < 0.001$) and the restored (1.4 ± 2.5; $p < 0.001$) sites. No significant difference was found between restored and reference sites (p = 1.0). The total abundance of invertebrates (Figure 6; Table 3) also differed significantly among the sites (Kruskal-Wallis $\chi^2(2) = 7.33$, $p < 0.05$, $\eta^2 = 0.014$). Post-hoc pairwise comparisons showed that the average invertebrate abundance was only different between the restored (25.9 ± 30.9) and the unrestored sites (15.6 ± 21.4, $p < 0.05$).

Environmental DNA

DNA Sequencing Output by Phyla

The dataset consisted of 3,981 ASVs and 1,350,202 total reads across all samples following sequence analyses and quality control filtering. A total of 35 eukaryotic phyla

were detected and assigned across Chromista (9 phyla), Plantae (4 phyla), Animalia (14 phyla), Fungi (4 phyla), and Protista (4 phyla; Figure S2). Of these kingdoms, Chromista was represented by the greatest number of both ASVs and untransformed sequencing reads 2,544 ASVs; 812,859 reads) — followed by Plantae (541 ASVs; 98,190 reads), Animalia (397 ASVs; 393,712 reads), and Fungi (295 ASVs; 23,698 reads). There were 8 ASVs (381 reads) that could not be assigned to the kingdom level.

Of the five phyla with the highest sampled ASV richness, four were Chromista: Bacillariophyta (1,613 ASVs; 623,144 reads), Ochrophyta (389 ASVs; 67,893 reads), Ciliophora (218 ASVs; 76,469 reads), and Oomycota (202 ASVs; 23,437 reads; Figure 7). Rhodophyta however had the second-greatest assigned ASV richness of any phyla (457 ASVs; 64,298 reads), accounting for the majority (84%) of ASVs assigned to the kingdom Plantae (Figure 7). Among metazoans: Cnidaria had the greatest ASV richness (174 ASVs; 10,920 reads), followed by Mollusca (67ASVs; 167,474 reads), Porifera (46 ASVs; 3,016 reads), Platyhelminthes (32 ASVs; 7,184 reads), and Arthropoda (26 ASVs; 35,279 reads; Figure S2). In terms of raw sequencing reads, Annelida was the third most abundant phyla among all kingdoms while being represented by low ASV diversity (8 ASVs; 153,520 reads; Figure 7).

ASV Richness by Site

ASV richness was evaluated in terms of both the overall site richness and the average number of ASVs observed per sample (Figure 8). Overall site richness reflects the total number of unique ASVs observed across all samples from each site, with each ASV counted only once, regardless of its presence in multiple samples (Figure 8A). The Restored site exhibited the highest overall richness, with 1,921 observed ASVs — 13.3% more ASVs than the number detected at the Reference coral community (1,696 ASVs) and 23.5% more than the sampled richness of the Unrestored seabed (1,555 ASVs). When excluding the Bacillariophyta ASVs — given the impact the disproportionately high diversity of this phylum may have on observed patterns of overall site richness — the Restored site still displayed the highest number of observed ASVs (1,129). In contrast, a greater number of non-Bacillariophyta ASVs were observed at the Unrestored site (1,003) than at the

Reference site (833). Non-Bacillariophyta richness at the Restoration site was therefore 12.5% higher than that of the Unrestored site and about 35.6% higher than that of the Reference site.

Across all three sites, an average richness of 1,130 ASVs per sample was observed (± 255 *SD*, *n* =14). The Restored site showed the highest average sample richness at 1,280 ASVs (± 284 *SD*, *n* = 5), followed by the Reference site at 1,125 ASVs (± 129 *SD*, *n* = 5), and the Unrestored site, which had the lowest average sample richness of 948 ASVs (± 266 *SD*, *n* = 4). Greater variation in ASV richness was observed among samples collected from the Unrestored and Restored sites than among those from the Reference coral community (Figure 8 B). Considering the relative differences in mean sample richness between sites, ASV richness from the Restoration site was 13.7% greater than that of the reference community, and 35% higher than that of the unrestored site. However, the results of a one-way ANOVA of ASV richness by site indicate that the differences in sample ASV richness between sites were statistically insignificant ($F(2, 11) = 2.225$, $p > 0.1$; Table 6).

Community Similarity

Most ASVs were unique to an individual site, as 76% of all ASVs were exclusively found among samples from one of the three locations (Table 5). A similar number of site-specific ASVs were found at the Restoration site (1,059; 27% of all ASVs) and the Reference site (1,064; 27%). In contrast, the Unrestored site had a lower number of site-specific ASVs than the other two sites, with only 880 site-specific ASVs (22% of all ASVs). Among ASVs that were shared between only two sites, the Restoration site shared a slightly higher number of ASVs with the nearby Unrestored seabed (341 ASVs; 9% of all ASVs) than with the Reference coral community (303 ASVs, 8% of all ASVs). However, the Unrestored site had far fewer ASVs in common with the Reference site (121 ASVs; 3% of all ASVs).

Only 213 ASVs were identified across all three sites (Table 5). While these ubiquitous ASVs accounted for a small share (5%) of all observed ASVs, they were represented by a relatively large number of reads, accounting for 23% of Hellinger-transformed read counts across all samples. The majority of these ubiquitous ASVs were

Bacillariophyta (123 ASVs; 57 of all ubiquitous ASVs), followed by Ochrophyta (21; 10%), Ciliophora (12; 6%), and Rhodophyta (11; 5%). All other phyla were represented by fewer than 10 ubiquitous ASVs.

Two sets of Principal Coordinate Analyses (PCoA) were conducted to assess differences in community composition between sites. Each site was shown to have a distinct community structure, with both ordinations producing tight, largely non-overlapping clusters (Figure 9). The Jaccard distance ordination (presence/absence) showed some overlap between the Unrestored and Restored sites along the first principal coordinate (PCo1, 31.5%). However, all three sites occupied distinct positions along the second principal coordinate (PCo2, 24.3%; Figure 9A). PERMANOVA analyses of the Jaccard dissimilarity matrix confirmed significant differences in assemblages between the sites ($F = 6.9$, $p < 0.001$; Table 7), with post-hoc pairwise testing indicating significant differences between all site pairs ($p < 0.01$; Table 8).

The Bray-Curtis distance analysis, which is calculated based on both occurrence and abundance, produced clear site clusters with minimal overlap. The Restored site plotted between the Unrestored and Reference sites on the first principal component (PCo1, 31.2%), while the Reference site again appeared centrally positioned between the other two on the second component (PCo2, 20.6%; Figure 9B). The PERMANOVA based on the Bray-Curtis dissimilarity matrix indicated statistically significant differences in community composition by site ($p < 0.001$; Table 7), with post-hoc tests confirming significant differences between all site pairs ($p < 0.05$ to 0.012; Table 8). In both ordinations, samples from the Reference site clustered more closely together than those from the other two sites (Figure 9). This effect was particularly pronounced in the Bray-Curtis ordination, suggesting that read count representation of individual ASVs was more consistent across samples from the Reference site.

Taxonomic Composition by Site: Diversity and Abundance

Given the wide taxonomic breadth of the sequencing data, it was only feasible to compare eukaryote community composition at the phylum level. Taxonomic composition was first assessed using presence–absence transformed data, illustrating the number of

ASVs observed within each phylum by site. ASV richness for each phylum was relatively consistent across the three sites, except for Bacillariophyta, which was represented by more ASVs and contributed a greater share of site richness at the Reference site (Figure 10). Of the 36 phyla identified, 25 were represented by at least 10 ASVs and were retained to test for variation in phylum ASV richness by site (Figure S2). This test confirmed a significant difference in phylum richness by site ($\chi^2 = 138.1$, $df = 48$, $p < 0.001$), primarily driven by differences in the number of Bacillariophyta observed between sites. Bacillariophyta ASV richness was highest at the Reference site (863 ASVs, 50.9% of site ASVs), lower at the Unrestored site (552 ASVs, 35.5%), and intermediate at the Restored site (792 ASVs, 41.2%). Across all three sites, Bacillariophyta contributed 34.6% to the calculated chi-square value, while no other phylum contributed more than 6%. Overall, Bacillariophyta accounted for 40.5% of all detected ASVs. Recognizing that the high diversity of Bacillariophyta may obscure richness patterns among other phyla, a second chi-square test was performed excluding Bacillariophyta ASVs. In this analysis, ASV richness by phylum was largely equal across sites ($\chi^2 = 138.1$, $df = 46$, $p = 0.101$). Cnidaria was the only potential exception, contributing 17.0% to the test statistic, and was slightly more diverse at the Reference (79 ASVs, 9.5% of all non-Bacillariophyta ASVs) and Restored (75 ASVs, 6.6%) sites than at the Unrestored site (58 ASVs, 5.8%).

The taxonomic composition of both individual samples and merged site communities was further examined using Hellinger-transformed read abundances. Across all sites, Bacillariophyta was the most abundant phylum, accounting for an average of 51.1% of all transformed read counts per sample (± 11.8% *SD*; Figure 11A). The next two most abundant phyla, Ochrophyta and Rhodophyta, were generally present in similar proportions, each representing approximately 8% of total transformed read counts per sample (8.3 ± 1.4% and 8.0 ± 1.5% *SD*, respectively; Figure 11A). Phylum-level read abundance was more consistent among replicates from the Reference community, mirroring the tighter clustering observed among Reference site samples in the Bray-Curtis ordination (Figure 9B). In contrast, there was substantial variation in phylum representation across samples from the Unrestored site. For the Restored site, variation in

phylum-level abundance was intermediate, with relative read abundance profiles for the seven most abundant phyla closely matching those of the Reference site. However, two samples from the Restored site had unusually high Mollusca read abundances (14.0% and 7.6% of total transformed reads).

Compositional abundance—presented as relative Hellinger-transformed abundance by site—was used as a proxy for site-level community composition. Bacillariophyta abundance varied considerably by site, with the highest compositional abundance at the Reference site (61.4%), followed by the Restored (50.9%) and Unrestored (38.4%) sites (Figure 11B), consistent with the gradient in Bacillariophyta richness observed across sites (Figure 10). As Bacillariophyta accounted for 53.7% of all transformed read counts across samples, patterns in compositional abundance for other phyla were obscured, prompting removal of Bacillariophyta from the dataset to better examine differences among remaining phyla.

Following Bacillariophyta, Ochrophyta and Rhodophyta were the most abundant phyla across all sites. For both algal phyla, compositional abundance was lowest at the Unrestored site, intermediate at the Restored site, and highest at the Reference site. In samples from the Unrestored, Restored, and Reference sites, respectively: Ochrophyta accounted for 13.5%, 17.7%, and 19.3%, and Rhodophyta for 14.8%, 16.5%, and 18.4% of non-Bacillariophyta transformed reads (Figure 11C). A similar gradient was observed for relative Cnidaria abundance, which was lowest at the Unrestored site (3.6%), higher at the Restored site (4.6%), and highest at the Reference site (7.5%; Figure 11C).

Other phyla displayed different patterns of compositional abundance between sites. Ciliophora abundance was relatively even across all samples, being slightly higher at the Unrestored (10.8%) and Restored (11.5%) sites than at the Reference site (9.9%; Figure 11C). In contrast, Basidiomycota was more abundant at the Reference site (7.1%) than at the Unrestored (5.5%) and Restored (5.0%) sites. Differences in relative Mollusca sequence abundance were more pronounced, being high at the Unrestored (6.7%) and Restored (9.5%) sites, but negligible at the Reference site (1.7%). Notably, Annelida accounted for a large share of transformed reads at the Unrestored site (9.0%), but

contributed minimally at the other two sites (<1.0%). Ascomycota sequences accounted for a greater share of reads from the Restored site (3.9%) than from the Reference (2.9%) or Unrestored (2.2%) sites.

Discussion

Coral restoration has two primary ecological goals, broadly: coral population enhancement, and the preservation of community biodiversity and ecosystem function. In this study, we developed and deployed a novel 3D-printed ceramic tile design to establish a coral community in a marine park in Hong Kong. Evaluation of the tiles' efficacy for coral reef restoration showed that the artificial structures provided a suitable substrate, supporting sustained coral growth and high survivorship of transplanted fragments. This, in turn, resulted in a measurable enhancement of site biodiversity.

Ecological Outcomes

Coral Performance

Our results demonstrate that the 3D-printed ceramic tiles provided a suitable substrate for coral attachment and growth. After four years, 91% of the 378 coral fragments outplanted to the restoration site remained alive, with only 2% showing signs of tissue loss. This survivorship rate significantly exceeded the average of 66% reported for coral transplantation projects—often considered an overestimate, as most studies monitor survivorship for only 18 months post-transplantation (Boström-Einarsson et al., 2020; Hein et al., 2017). Our project met the suggested targets of the Coral Restoration Consortium (CRC) of the National Oceanic and Atmospheric Administration (NOAA), whose Restoration Evaluation Tool provides the only comprehensive suite of quantitative targets for evaluating coral reef restoration performance.

The CRC recommends the following criteria for coral health and survivorship, measured one year after transplantation: (1) high coral survivorship (>80% of outplanted fragments alive), (2) high mean live tissue coverage (>80% per colony), (3) limited coral bleaching (<5% of fragments with tissue loss due to bleaching), and (4) low disease prevalence (<10% of fragments showing disease; Goergen et al., 2011). At the one-year mark, all criteria were met: only one fragment died, and five detached, resulting in an overall survivorship rate of 98%. While the exact percentage of tissue loss per fragment

was not quantified, 98% of fragments exhibited full tissue cover, suggesting mean live tissue coverage exceeded 80%. Diver surveys using color indices found no signs of coral bleaching or disease. The CRC's longer-term targets for survivorship are >65% cover for years 2–5 post-transplantation and >50% thereafter. Although our monitoring covers only the first four years, the high final survivorship and minimal losses over time suggest the project will continue to meet these criteria, barring unforeseen acute stress events.

Coral growth rates can vary considerably among species and morphologies, with branching corals generally growing faster than massive and plating forms (Gladfelter et al., 1978; Zawada et al., 2019). Consistent with expectations, we observed the fastest growth in *Acropora* (0.35 cm/month), followed by *Pavona* (0.21 cm/month) and *Platygyra* (0.15 cm/month) over four years. These rates align with their growth forms, as branching corals are structurally adapted for rapid growth (Rossi et al., 2018). However, growth rates are highly context-specific due to environmental factors such as temperature, light, water quality, nutrients, salinity, and aragonite saturation (Lough and Barnes, 2000; Browne, 2012). The CRC does not specify growth rate targets, instead using increased mean coral height or linear extension as a measure of enhanced reef structure (Goergen et al., 2020). Our project met this criterion, with the mean maximum linear extension of all three genera at least doubling.

Acropora is often favored for restoration due to its high growth rates and branching morphology, which enhances structural complexity (Calle Trivino et al., 2021; Young et al., 2012). In our study, *Acropora* achieved the highest survivorship, albeit with a higher incidence of breakage compared to *Pavona* and *Platygyra*. This is consistent with the ecological strategies of branching corals, which are adapted to high-disturbance environments and can recover quickly through fragmentation (Highsmith, 1982; Lirman, 2000). However, the high survivorship of *Acropora* observed here is atypical; literature often reports higher mortality rates for transplanted *Acropora*, reflecting a tradeoff between growth and survivorship (Clark and Edwards, 1995; Goergen et al., 2020; Yap et al., 1992; Ware, 2020).

Transplanting diverse coral assemblages offers ecological advantages, as fast-growing branching species like *Acropora* can offset predation and disturbance pressures on slower-growing taxa, facilitating their establishment (Caibatan et al., 2015). Massive and foliose corals tend to be more resistant to environmental stressors, contributing to long-term stability (Caibatan et al., 2015). Functional diversity also enhances community-level resilience, with mixed assemblages of autotrophic and heterotrophic species conferring increased resistance to thermal bleaching (Conti-Jerpe et al., 2020). This approach is especially relevant in urbanized, eutrophic environments such as Hong Kong, where heterotrophic taxa may be more resilient under nutrient enrichment (Duprey et al., 2018; Cybulski et al., 2020).

Despite these benefits, implementing species-diverse outplanting strategies presents challenges, particularly in optimizing attachment techniques for different morphologies. In our study, most fragment losses resulted from detachment, with *Pavona* (a plating coral) being disproportionately affected. This highlights the need for attachment methods tailored to specific growth forms to maximize survivorship and overall restoration efficacy. Addressing these technical considerations will enhance the ecological benefits of species and functional diversity, increasing the resilience and sustainability of restored communities. In summary, our monitoring demonstrates that 3D-printed ceramic tiles provide a suitable substrate for coral attachment and growth. However, while substrate is important, appropriate site selection ultimately determines coral survivorship outcomes.

Biodiversity

Fish and Macroinvertebrate Abundance

A key consideration in the tile design was to create artificial structure that attracts and supports a diverse marine community. Fish, due to their economic and nutritional value, have long been the focus of studies on artificial reefs (Bohnsack and Sutherland, 1985; Higgins et al., 2022). Numerous studies show that artificial structures attract abundant and diverse fish assemblages (Arena et al., 2007; Gratwicke and Speight, 2005; Santos et al., 2005; Sherman et al., 2002). In this study, visual surveys found an average of seven times more fish at the restoration site than at the nearby unrestored seabed, with

abundances comparable to those at the natural reference coral community. Macroinvertebrate abundance similarly differed between sites, with 45% greater abundance of sea urchins and sea cucumbers at the restored site than at the unrestored area.

Moderate densities of sea urchins and small herbivorous fishes on and near the tiles are a promising sign for restoration success. Herbivory is critical for maintaining coral ecosystems, especially in eutrophic environments like Hong Kong, where high nutrient levels otherwise favor turf algae that can outcompete corals and reduce biodiversity (Burkepile and Hay, 2008; Hughes et al., 2007; Mumby & Steneck, 2008). While moderate sea urchin densities control macroalgae, excessive densities can harm corals (Glynn & D'Croz, 1990; Carreiro-Silva & McClanahan, 2012). In our surveys, urchin densities at the restoration and reference sites were comparable, appearing compatible with coral growth. Looking beyond herbivory, the surveyed fish taxa included representatives of different trophic levels — sweetlips (Plectorhinchus spp.) that feed on shrimp and small crabs, wrasse (Labridae) which prey on larger invertebrates such as sea urchins and mollusks, and groupers (Epinephelinae) known to feed on other reef fish, octopuses, and larger crustaceans. The presence of fish reliant on a diversity of feeding strategies suggests that the restored habitat is supporting a functioning trophic network. From a socioeconomic perspective, the presence of commercially valuable species such as groupers also enhances the potential for local community engagement and the economic viability of restoration efforts.

Our results meet the CRC's criterion for non-coral community biodiversity enhancement, which requires greater abundances of fish and coral grazers at the restoration site relative to a control. However, whether increased fish and macroinvertebrate abundance reflects true enhancement of local carrying capacity, or simply aggregation around new habitat, is uncertain. This distinction is especially relevant for mobile species such as fish (Boström-Einarsson et al., 2020; Gratwicke & Speight, 2005).

Without pre-restoration biodiversity data, we cannot determine whether elevated abundances at the restoration site are due to local recruitment and population growth, or simply redistribution from less-structured areas. Nevertheless, aggregation may still enhance ecosystem resilience by concentrating functional groups like herbivores, supporting key ecological processes even if overall population sizes remain unchanged (Olds et al., 2012). Visual surveys are effective for large, mobile taxa, but often underrepresent cryptic or small-bodied species (MacNeil et al., 2008). Thus, more comprehensive and temporally resolved surveys — including pre-installation baselines and complementary methods such as environmental DNA — are needed to robustly assess biodiversity and carrying capacity impacts.

eDNA Cryptobiome

Environmental DNA (eDNA) metabarcoding provided a powerful tool to examine the ecological consequences of adding artificial substrate to a previously barren sandy seafloor across a wider range of taxa. The restored site supported substantially higher eukaryotic richness (1,921 ASVs) compared to the unrestored seabed (1,555 ASVs), representing a 23.5% increase. Even after excluding Bacillariophyta, whose hyperdiversity can obscure patterns, the restored site still exhibited the highest richness (1,129 ASVs), 12.5% greater than the unrestored site. Additionally, more unique ASVs were found at the restoration site than at the unrestored seabed (1,059 and 880 ASVs, respectively). Beta diversity analyses further supported these findings, with both Jaccard and Bray-Curtis ordinations revealing tight, non-overlapping clusters and PERMANOVA confirming significant differences in community composition between the restored and unrestored sites ($p < 0.001$). These results demonstrate that substrate addition, combined with coral outplanting, can rapidly generate novel eukaryotic assemblages.

To pour knowledge, this study represents both the first use of eDNA in monitoring a reef restoration project, and the only published coastal sedimentary eDNA dataset that focuses on eukaryote biodiversity. This lack of precedent makes it difficult to contextualize the magnitude of the observed effect sizes. Nevertheless, ecological theory and empirical evidence emphasize that elevated taxonomic richness enhances ecosystem resilience and

functional stability, even if much of the diversity is functionally redundant (Yachi & Loreau, 1999; McGrady-Steed et al., 1997; Naeem & Li, 1997). The fact that 76% of ASVs were unique to a single site, and that community structure diverged so sharply with restoration — despite the close spatial proximity of the sites — suggests that artificial substrate provision can serve as a potent driver of local biodiversity. However, our findings are limited by the single timepoint sampling (two years post-deployment), likely reflecting only one stage in ecological succession. Artificial reef communities are known to undergo dynamic changes over years (Perkol-Finkel & Benayahu, 2005), and the temporal and spatial variability of eDNA in marine sediments remains poorly characterized (Beng & Corlett, 2020). Future studies should incorporate pre-deployment baselines and annual monitoring to capture the trajectory of succession and the persistence of these patterns.

A key consideration in interpreting richness and community assembly at the restoration site is the interplay between structural complexity and biological augmentation. The structural complexity of the tile surfaces, together with the ongoing growth of transplanted coral fragments, likely increased both habitat complexity and resource availability. Such complexity is widely recognized as a determinant of both macro- and microfaunal diversity in reef systems (Gratwicke & Speight, 2005; Sherman et al., 2002). Our results support the view that holistic restoration approaches — those that foster habitat for cryptic and encrusting taxa as well as corals — can maximize biodiversity gains and ecosystem functioning. The Restored site's community was not simply a reflection of transplanted coral, but rather a mosaic shaped by the combined effects of added substrate and benthic colonization by diverse eukaryotic lineages.

Evidence for convergence between the restoration and reference sites — such as comparable richness and increased abundance of key taxa — was tempered by findings that the restored and unrestored sites continue to share certain community characteristics distinct from the reference reef. Richness at the restored site (1,921 ASVs) exceeded that of the reference reef (1,696 ASVs), and the two sites shared a similar proportion of unique ASVs (~27% each). In terms of taxonomic composition, both presence-absence and abundance data revealed gradients: foundational groups such as

Bacillariophyta, Rhodophyta, Ochrophyta, and Cnidaria were most abundant at the reference site, intermediate at the restored site, and least abundant at the unrestored site. These findings suggest that well-designed restoration interventions can augment the seascape with new ecological niches, supporting the broader objective of enhancing overall ecosystem resilience (Gann et al., 2019; Rossi et al., 2018).

Measuring Coral Restoration Outcomes

The most commonly stated objective among peer-reviewed coral reef restoration studies—whether conducted on existing reefs or in areas augmented with artificial structures—is the establishment of a self-sustaining, functioning coral reef ecosystem (Hein et al., 2017). While the majority of studies articulate broad ecological goals such as preserving ecosystem functions, enhancing biodiversity, and fostering resilience, a review by Boström-Einarsson et al. (2020) found that 45% of projects with ecological objectives failed to collect relevant measurements to evaluate them. Across the literature, there is a disconnect between the ecological aspirations of restoration projects and the indicators used to measure success, with fragment-scale measures of coral growth and survivorship reported far more frequently than community-level composition metrics (Hein et al., 2017; Bayraktarov et al., 2019). Even among studies that include coral-associated community surveys, fish are often the sole taxa reported (~60%; Higgins et al., 2022). Recent eDNA-based monitoring of reef restoration also reflects this bias: with one exception, prior work has focused primarily on fish populations (Sato et al., 2021; Inoue et al., 2022; Krolow, 2019; Krolow et al., 2022; Miyajima-Taga et al., 2024).

Levy et al. (2023) published the first example of eDNA being used to detect a broad range of metazoan taxa settling on or near artificial structures in a marine environment, demonstrating the promise of eDNA for capturing the often-overlooked diversity of reef-associated organisms. Building on this work, our study is the first to use eDNA metabarcoding to assess how coral reef restoration influences eukaryote diversity. By including both restored and control sites, our approach enables a direct comparison of biodiversity outcomes attributable to restoration interventions—an advancement over previous studies, which typically report the community that has settled on new structures

without baseline or control site assemblages for comparison. To our knowledge, Knoester et al. (2023) represent the only other example of a benthic biodiversity survey comparing communities associated with artificial reefs to a relevant control site; their visual surveys of several macroinvertebrate groups revealed different effects on abundance but could not resolve an overarching effect on site-wide biodiversity. Our survey therefore represents the first evidence of a community-wide enhancement of site richness associated with a coral restoration project.

A major strength of using eDNA for coral ecosystem monitoring is its ability to detect a broad suite of taxa, including cryptic and sessile organisms such as crustose coralline algae (CCA) and sponges (Levy et al., 2023). These groups are increasingly recognized for their beneficial roles in coral recruitment, ecosystem engineering, and overall reef resilience (Harrington et al., 2004; Webster et al., 2011). By capturing this wider spectrum of biodiversity, eDNA offers a more holistic perspective on the ecological outcomes of restoration interventions. However, several limitations must be acknowledged. The replication and temporal resolution of our eDNA sampling were constrained, limiting our ability to assess temporal trends or establish causality. More broadly, the novelty of eDNA applications in reef restoration means that there are few comparable datasets, complicating interpretation and benchmarking of restoration success. Additionally, questions remain about the ecological significance of eDNA detections, as the method can recover signals from transient or low-abundance taxa whose functional roles within the ecosystem are unclear (Bessey et al., 2022).

Despite these challenges, eDNA provides a valuable foundation for developing more nuanced functional indices. While our study focused on biodiversity as an endpoint, eDNA data could also be leveraged to infer aspects of trophic complexity—an attribute increasingly recognized as central to ecosystem functioning and resilience (Gann et al., 2019). Moreover, eDNA can inform on the presence and relative abundance of foundational versus non-native species, and track functional groups relevant to nutrient cycling, reproductive outputs, and habitat stratification. Realizing the full potential of these molecular tools will require further experimental validation and integration with other

monitoring approaches, but our findings demonstrate the capacity of eDNA to advance the field toward more comprehensive and ecologically relevant assessments of coral reef restoration outcomes.

Conclusions

Our monitoring efforts demonstrate that the restoration project satisfied, and indeed exceeded, all relevant CRC evaluation criteria satisfied all measured CRC restoration objectives. The 3D-printed ceramic tiles provided a stable substrate for coral survivorship and growth, and supported higher abundances of key fish and macroinvertebrates. Furthermore, we demonstrate that sedimentary eDNA analyses can be used to effectively detect previously unmeasured changes in sitewide biodiversity, finding evidence that the tile deployment and coral transplantation supported increased eukaryote biodiversity at the restoration site. These results suggest that the restoration project was successful and support the potential for future use of these tiles as artificial substrates for coral restoration.

Figures

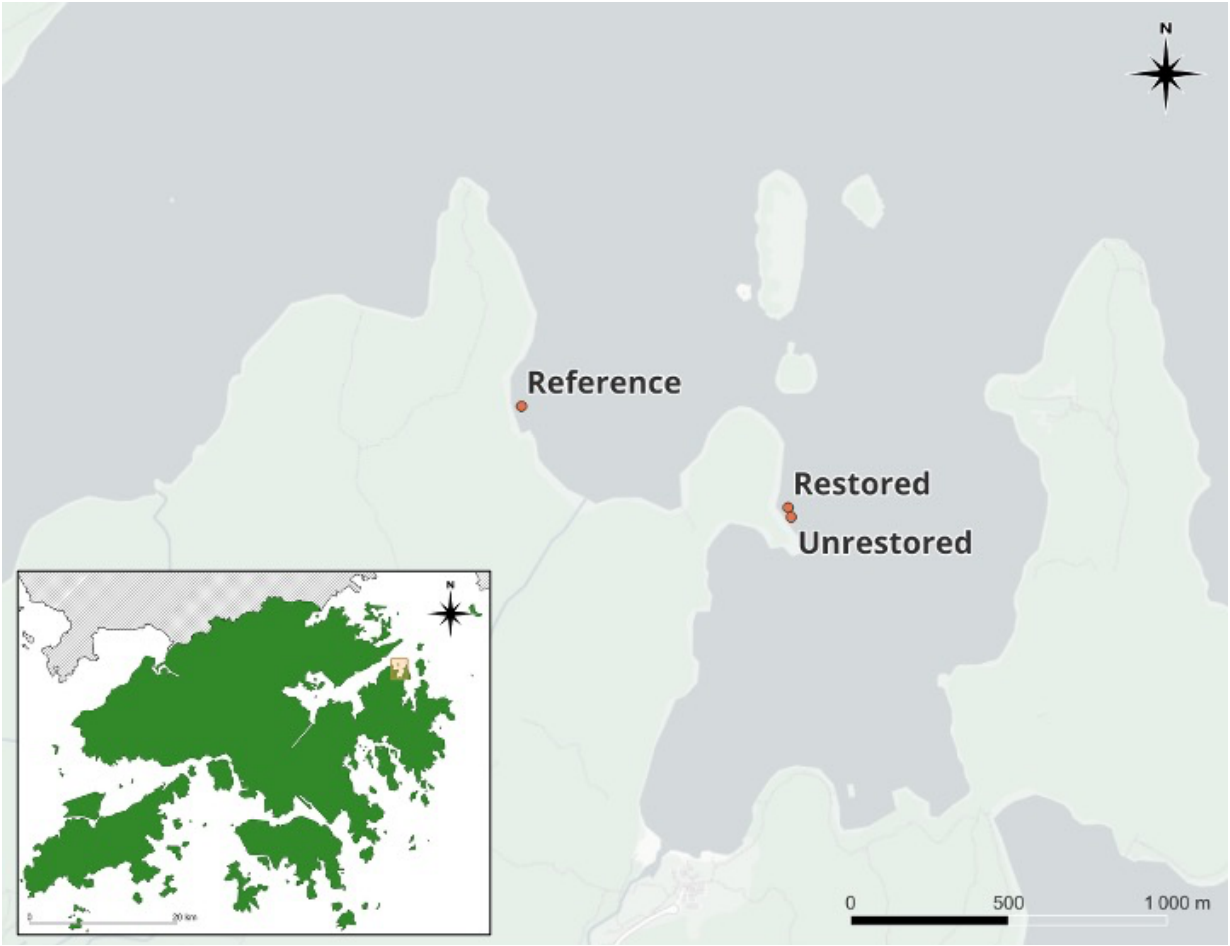

Figure 1: Locations of study sites in Hoi Ha Wan Marine Park, Hong Kong.
Map showing the positions of the Reference (Gruff Head), Restored (Coral Beach), and Unrestored (Coral Beach) sites surveyed in this study. Basemap data from © OpenStreetMap contributors and © CARTO, accessed via the QuickMapServices plugin in QGIS.

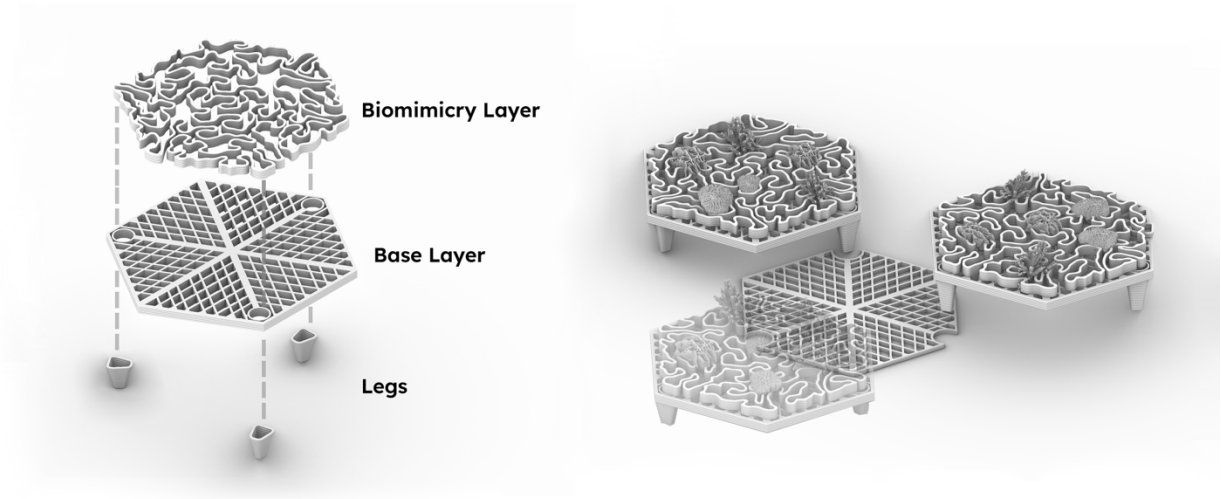

Figure 2: Design and structural components of the custom-engineered 3D-printed reef tiles used for coral recruitment and restoration
(Left) The upper "biomimicry layer" of the tiles features a biomimetic surface designed to mimic reef complexity, providing habitat for cryptic invertebrates. The grid layer has a diagrid framework and lateral bracing to enhance mechanical strength, reduce fabrication defects, and support uniform drying and firing. The integrated three-legged footing system is printed and attached post-processing to elevate the tile above the seabed, improving hydrodynamic flow and minimizing sediment accumulation. (Right) One assembled unit showing three tiles, onto which coral fragments were transplanted, anchored on one Base Layer plate. 24 of these assembled units were deployed in 5 m intervals along a 3x8 unit grid at the Restoration Site (Lange et al., 2020; Baker et al., 2022).

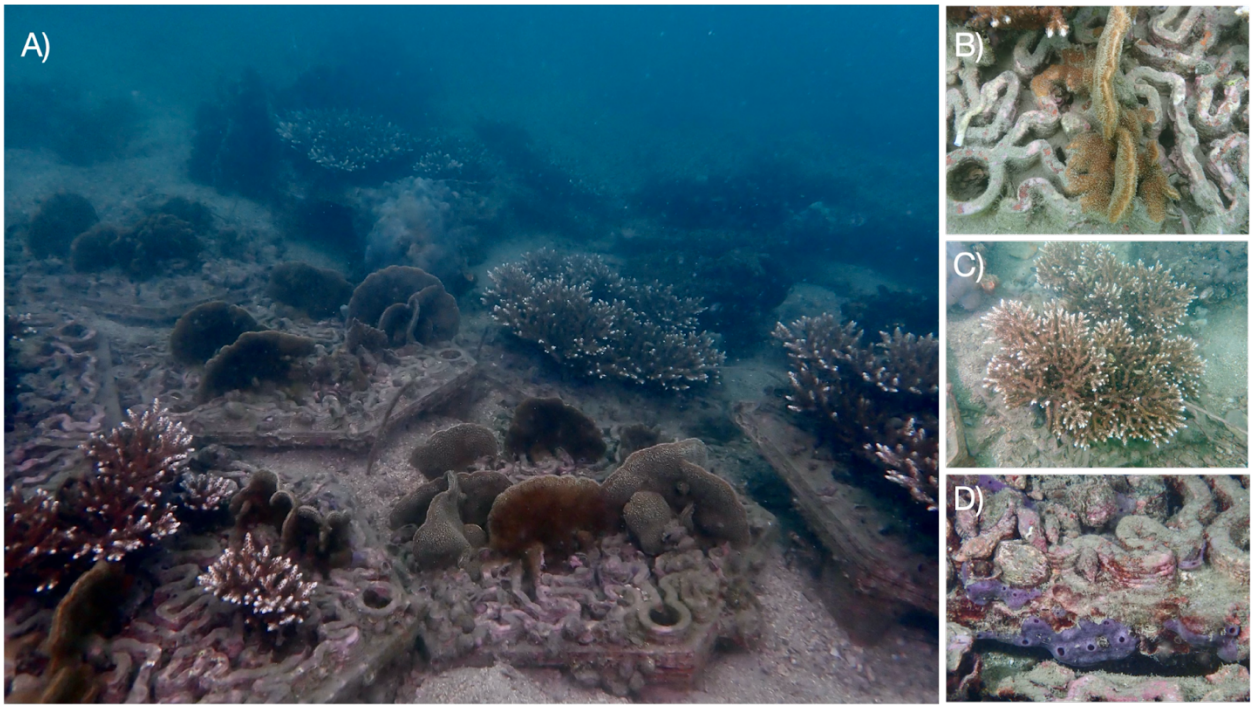

Figure 3: Composite image of the restoration project, 4 years after deployment
A) A subset of the ceramic reef tiles deployed at the restoration site in Hoi Ha Wan Marine Park, outplanted with multiple coral species representing branching, plating, and massive colony morphologies. B) Self-attachment of a transplanted fragment via new growth onto the biomimicry layer. C) A tile seeded with *Acropora* fragments, which have grown to obscure the existence of the reef tile below. D) Encrusting taxa that have grown onto the terra cotta surface of the reef tile, including marine sponges and coralline algae.

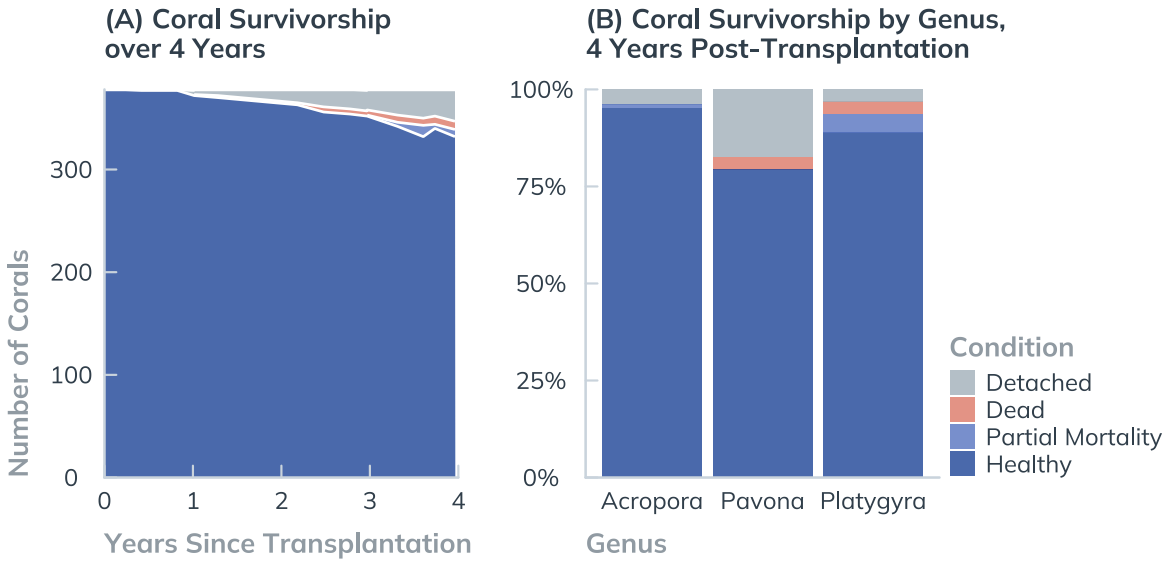

Figure 4: Summary of coral survivorship and condition
(A) The overall survivorship of corals, and (B) genus-specific survivorship of *Acropora* (red), *Pavona* (green), and *Platygyra* (blue) over a 4-year period following transplantation. Different conditions were recorded as Healthy (blue), Partial Mortality (light blue), Dead (red), and Detached (grey).

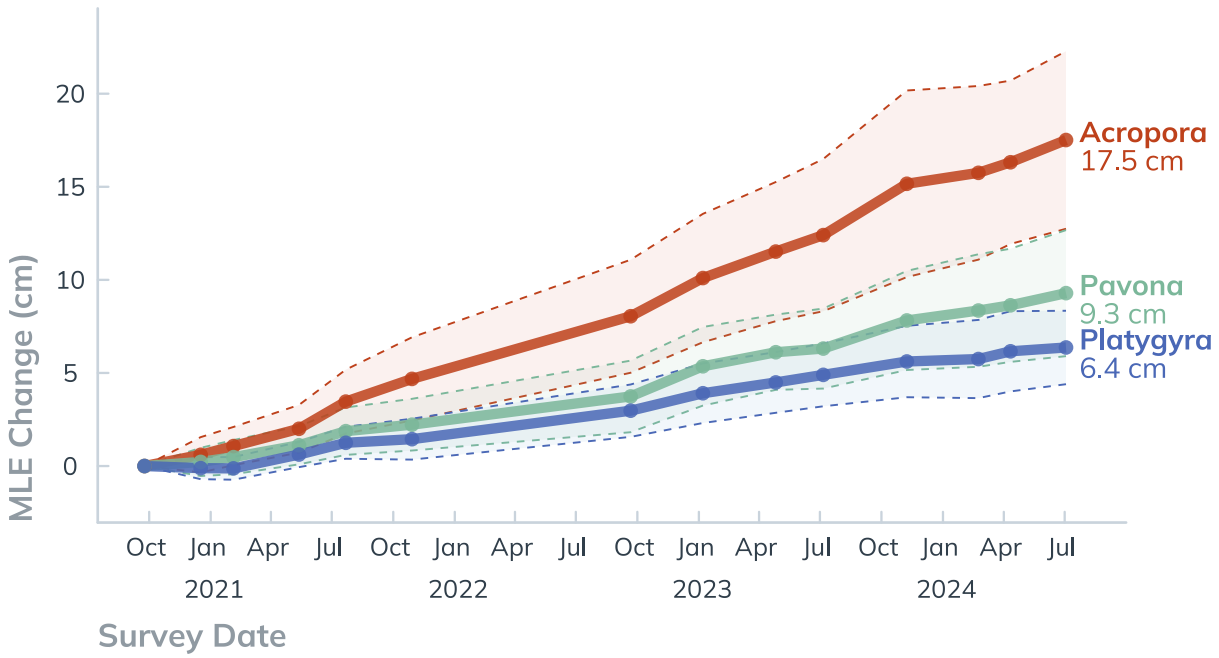

Figure 5: Coral Growth from transplantation size
Change in maximum linear extension (MLE, cm) of the three genera of corals, *Acropora* (red), *Pavona* (green), and *Platygyra* (blue) over a 4-year period following transplantation. The solid line represents the mean values; the dotted lines indicate standard deviation.

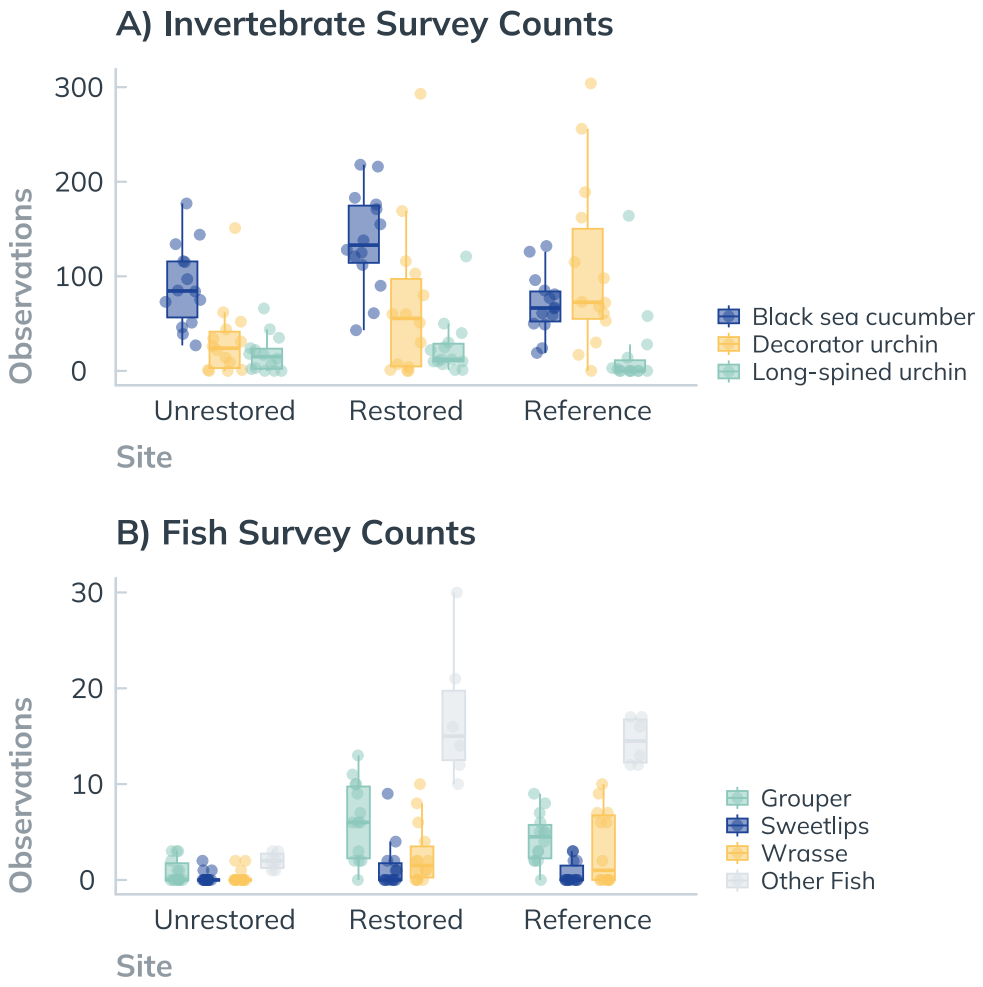

Figure 6: Visual survey counts
Each point represents the total number of observations of each bioindicator recorded during a single monitoring event for: A) Invertebrates and B) Fish.

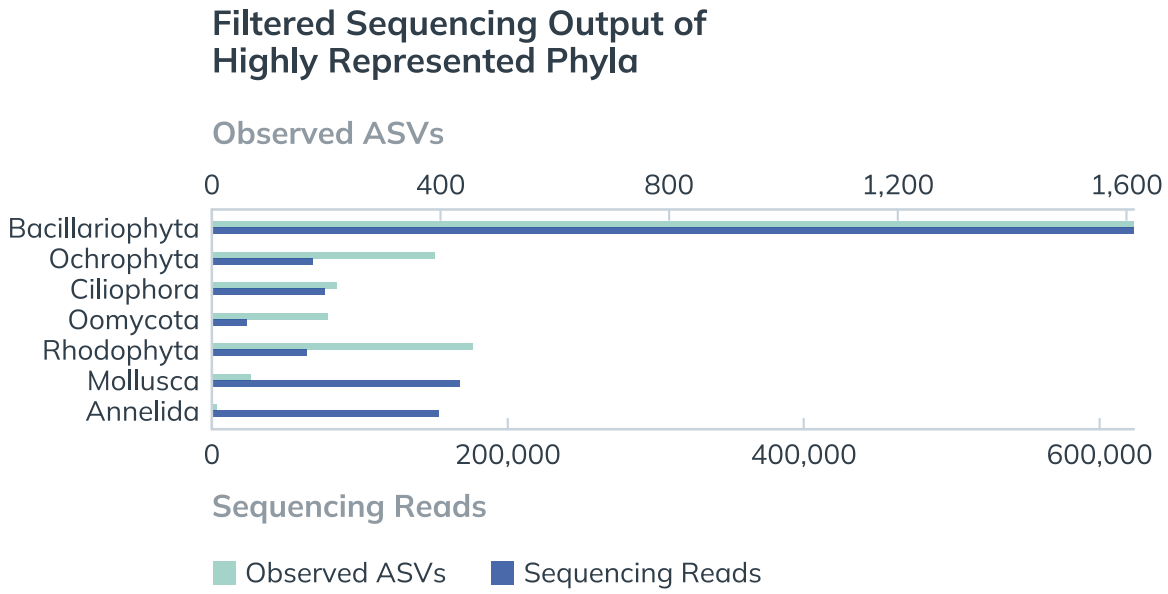

Figure 7: The number of observed ASVs and sequencing reads by phylum across all samples
Data shown reflects only those ASVs and reads which passed the prevalence and abundance filters prior to Hellinger transformation. For enhanced visibility, only the five phyla with the greatest ASV diversity (Bacillariophyta, Ochrophyta, Ciliophora, Oomycota, Rhodophyta) and/or the five phyla with the highest raw sequencing read counts (Bacillariophyta, Mollusca, Annelida, Ciliophora, Ochrophyta) were plotted.

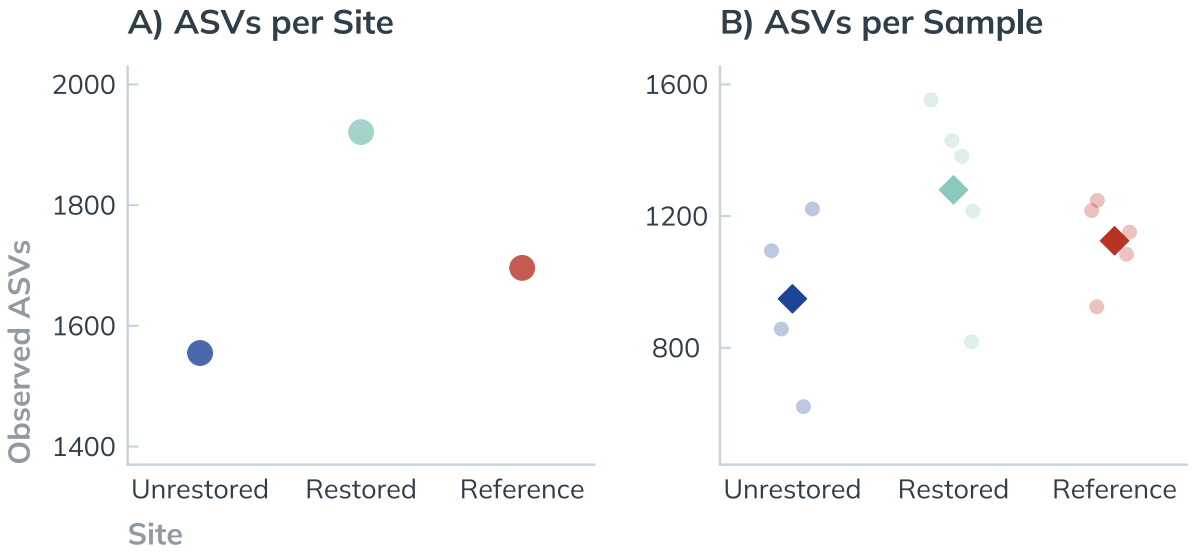

Figure 8: Point plots of observed ASV richness by site and per sample.
Based on the parameters of the prevalence filter applied to the community metabarcoding dataset, all ASVs represented in this plot appeared in a minimum of three samples per site. (A) The number of unique ASVs observed across all samples from the Unrestored (1,555 ASVs, $n = 4$), Restored (1,921 ASVs, $n = 5$), and Reference (1,696 ASVs, $n = 5$) site. Each ASV was counted once per site, regardless of how many replicates it was detected in. (B) The number of ASVs detected per sample are indicated by the circular points. Diamonds indicate mean ASV richness across all replicates for each site: 946 ± 266 ASVs per sample (±*SD*) from the Unrestored ($n = 4$), 1,280 ± 284 from the Restored ($n = 5$), and 1,125 ± 129 from the Reference ($n = 5$) site.

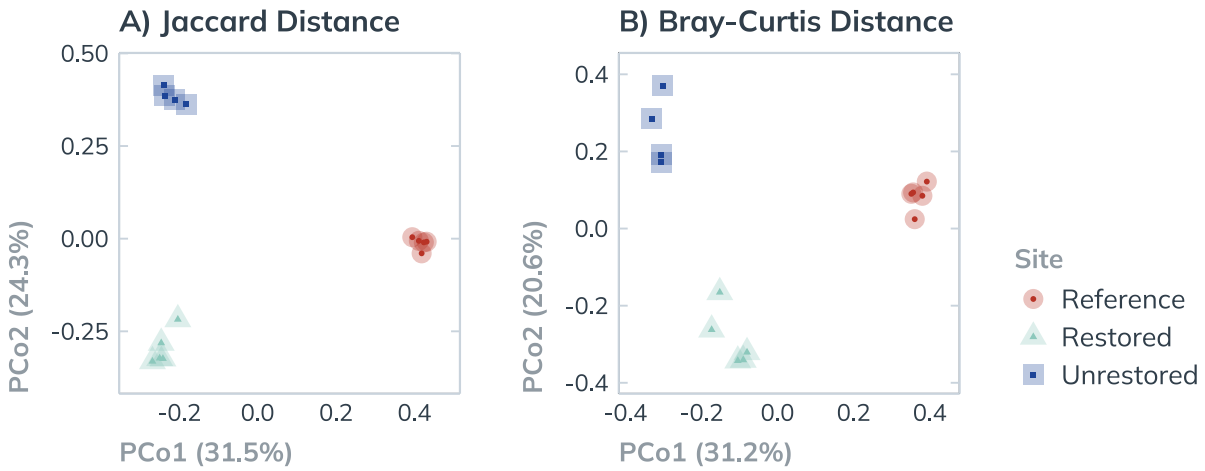

Figure 9: Beta diversity of eukaryotic ASVs.
Dissimilarity in community composition was measured by community dissimilarity matrices. Each point represents a single sample, sites are distinguished by color and shape (A) PCoA ordination based on Jaccard distance, a presence-absence based metric. (B) PCoA based on Bray-Curtis distance, which incorporates abundance data (Hellinger-transformed).

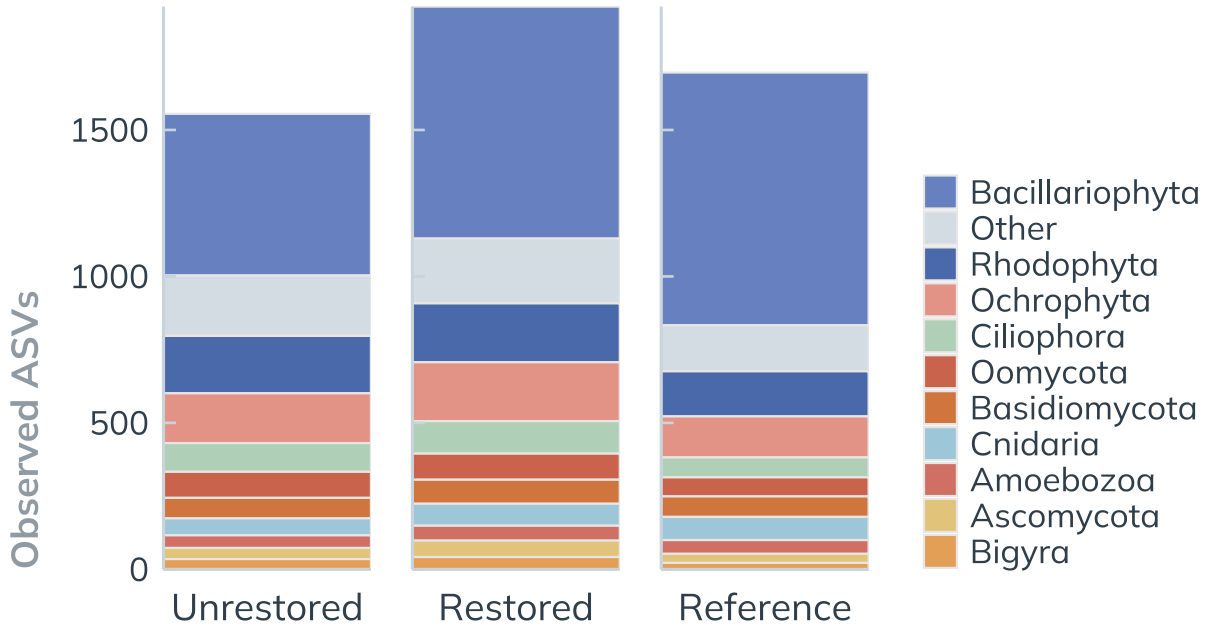

Figure 10: Eukaryotic phylum richness, by site.
Each bar represents the total number of ASVs observed across samples from each site, separated by color to depict phylum-level ASV richness. Bars are colored to indicate the 10 most diverse phyla within the eDNA COI metabarcoding dataset. “Other” represents the sum of observed ASVs that belong to the remaining 15 phyla.

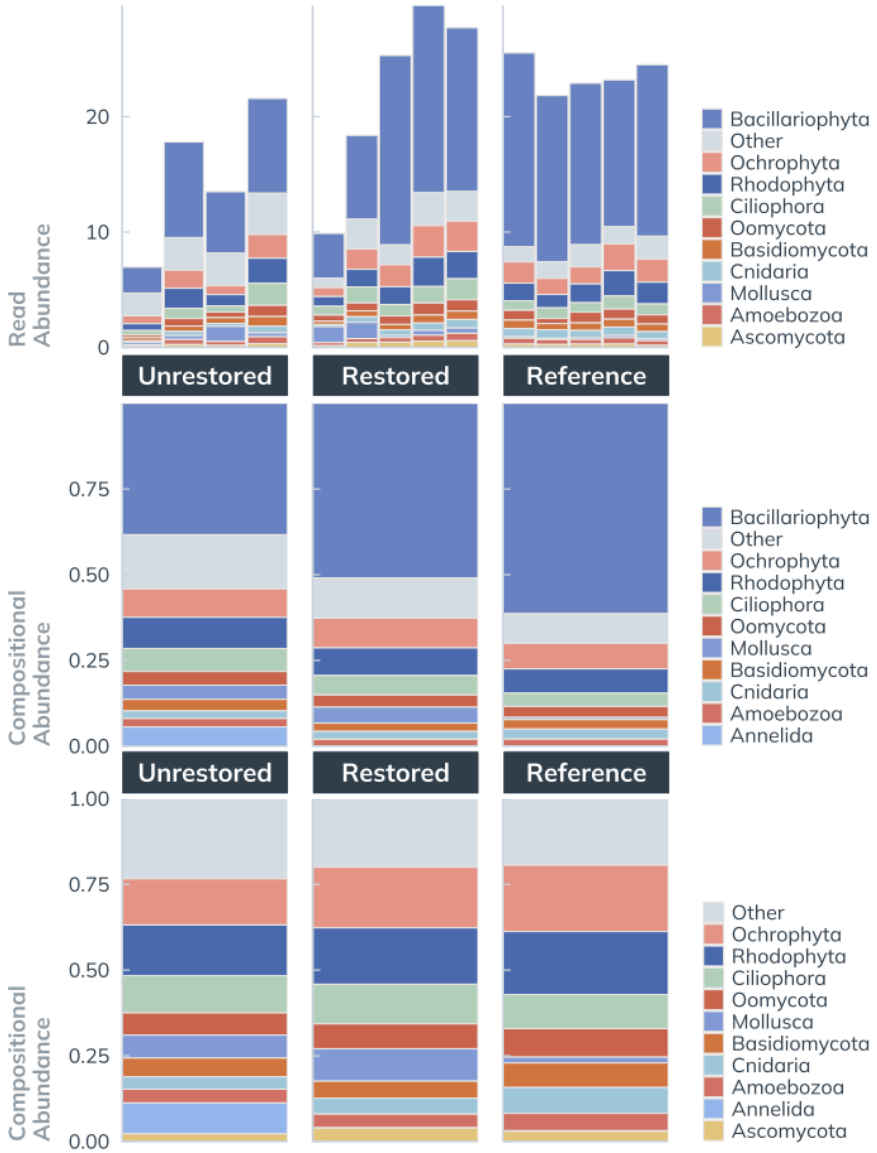

Figure 11: Taxonomic Composition by Phyla, based on Hellinger-Transformed Read Abundance. For each panel, the ten most abundant phyla are given distinct colors, while less abundant phyla have been merged as "Other". Each phylum is depicted with the same color across all panels, but the ten most abundant phyla vary by panel as a result of differences in how data for each was processed (Top: A) Stacked bar plot depicting the total Hellinger-transformed read abundance for each sample sample. (Middle: B) Read abundances were merged by site prior to Hellinger transformation, and subsequently converted to Compositional Abundance, to show the relative contribution of each phylum to the composite sequenced community for each site. (Bottom: C) Bacillariophtya ASVs were removed prior to merging by site and Hellinger transformation, to more clearly depict differences in the proportions of non-Bacillariophyta reads assigned to other phyla between sites.

Supplemental Figures

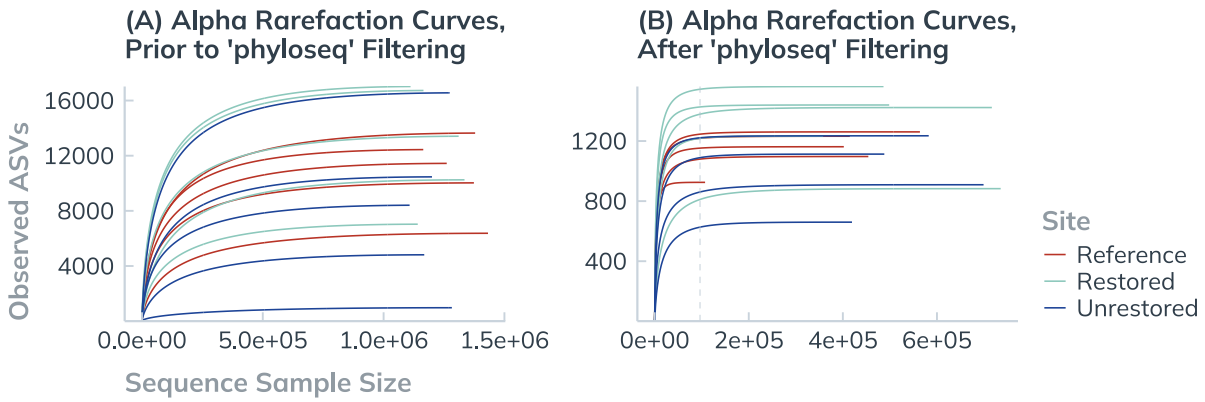

Figure S1: Rarefaction curves for ASV detection
Each line represents a sample, colored by site. (A) Rarefaction curves for ASVs inferred from the DADA2 *denoise-paired* function, before any subsequent cleanup steps. These curves indicate that the sequencing effort provided sufficient coverage for the taxa represented in the samples. The sample from the Unrestored site that was subsequently excluded from analyses based on abnormally low richness (974 ASVs) and biased taxonomic composition is shown. (B) Rarefaction curves plotted from the phyloseq object that resulted following prevalence and abundance filtering, which retained only those ASVs that appeared in at least three samples from the same site and were represented by a minimum of 50 reads. The dotted grey line indicates the sampling depth used for rarefaction (96,443 reads), which was set to 90% of the depth of the sample with the fewest reads.

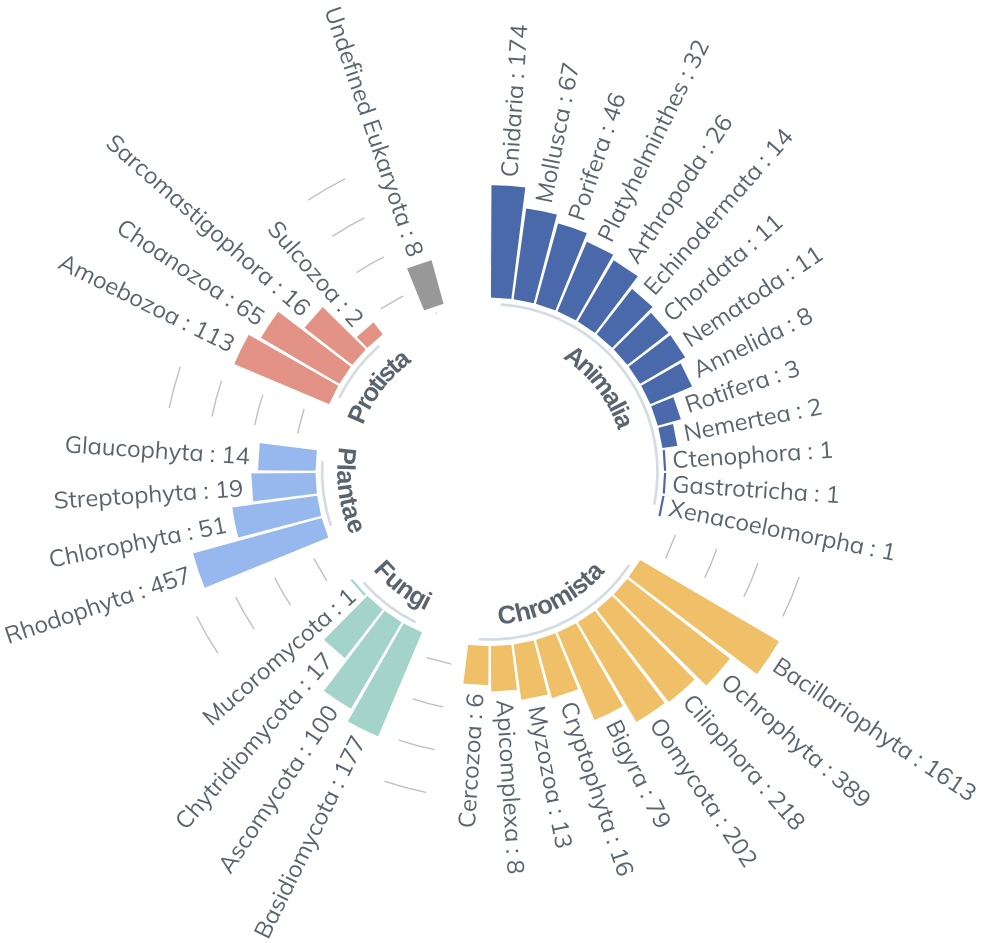

Figure S2: ASVs observed per phyla
Bar size and the number associated with each phylum name indicates the number of unique ASVs assigned to that phylum across all fourteen samples from all three sites. Phyla are grouped by kingdom, following the taxonomic used by the World Register of Marine Species (WoRMS) database. Logarithmic transformation was applied to the scale to enhance visibility.

Tables

Table 1: Bioindicator fish and invertebrate species monitored during surveys

Fish		Invertebrate	
Common Name	**Scientific Name**	**Common Name**	**Scientific Name**
Grouper	*Epinephelinae*	Long-spined sea urchin	*Diadema setosum*
Wrasse	*Labridae*	Decorator urchin	*Salmacis sphaeroides*
Sweetlips	*Plectorhinchinae*	Sea cucumbers	*Holothuria leucospilota*
Seahorse	*Hippocampus*		

Table 2: Results of pairwise mean comparisons of the estimated marginal means (EMMs) for coral genera effect

p-values have been adjusted using the Tukey method for multiple comparisons, ≤ 0.05 are highlighted in bold. est, estimate; SE, standard error; df, degree of freedom. A = *Acopora*, Pv = *Pavona*, Pt = *Platygyra*.

Survivorship	**SE**	**df**	**z.ratio (glmer)**	**Pairwise comparisons (*p*-values)**
A - Pv	0.233	Inf	-9.652	**< 0.0001**
A - Pt	0.270	Inf	-2.516	**0.0318**
Pv - Pt	0.176	Inf	8.897	**< 0.0001**
Detachment			**t.ratio (glm)**	
A - Pv	0.006	168	-11.173	**< 0.0001**
A - Pt	0.003	168	-1.522	0.3411
Pv - Pt	0.007	168	9.939	**< 0.0001**
Breakage			**t.ratio (glm)**	
A - Pv	0.141	168	18.111	**< 0.0001**
A - Pt	0.157	168	21.410	**< 0.0001**
Pv - Pt	0.015	168	3.541	**0.0015**
Extension			**z.ratio (glmmTMB)**	
A - Pv	0.063	Inf	8.437	**< 0.0001**
A - Pt	0.063	Inf	14.324	**< 0.0001**
Pv - Pt	0.063	Inf	5.752	**< 0.0001**

Table 3: Total abundance of bioindicator sightings across 14 surveys, and the mean count and standard deviation (SD) for each survey at the Reference, Restored, and Unrestored sites.

Site		Reference			Restored			Unrestored		
Bioindicator	**Type**	**Total count**	**Mean count**	**SD**	**Total count**	**Mean count**	**SD**	**Total count**	**Mean count**	**SD**
Grouper	Fish	61	4.4	2.6	87	6.2	4.0	13	0.9	1.3
Other Fish	Fish	87	14.5	2.4	103	17.2	7.3	12	2.0	0.9
Seahorse	Fish	0	0.0	0.0	0	0.0	0.0	0	0.0	0.0
Sweetlips	Fish	10	0.7	1.2	19	1.4	2.5	4	0.3	0.6
Wrasse	Fish	47	3.4	3.9	37	2.6	3.2	5	0.4	0.7
Black sea cucumber	Invert	992	70.9	32.6	1937	138.4	52.5	1263	90.2	43.3
Decorator urchin	Invert	1498	107.0	90.0	974	69.6	82.2	447	31.9	39.8
Long-spined urchin	Invert	269	19.2	44.8	351	25.1	31.1	251	17.9	19.5

Table 4: Results of the Kruskal-Wallis test comparing total abundance of fish and invertebrates between sites

p-values ≤ 0.05 are highlighted in bold. df, degree of freedom. Ref = Reference site, Res = Restored site, Un = Unrestored site.

Bioindicator group	Test statistic	df	*p*-value	*p*-value (Pairwise)
Fish	54.1	2	**< 0.0001**	Ref - Res: 1.0 **Ref - Un: < 0.0001** **Res - Un: < 0.0001**
Invertebrate	7.33	2	**0.0256**	Ref - Res: 0.364 Ref - Un: 0.752 **Res - Un: 0.0209**

Table 5: Unique, ubiquitous, and shared ASVs by site

		Observed ASVs	% of all ASVs	% of Reads	% of Reads
				Hellinger Transformed	*No Transformation*
Unique	Unrestored	880	22%	11%	18%
	Restored	1059	27%	14%	7%
	Reference	1064	27%	19%	13%
Shared	Unrestored -- Restored -- Reference	213	5%	23%	27%
	Unrestored -- Restored	341	9%	14%	19%
	Unrestored -- Reference	121	3%	5%	6%
	Restored -- Reference	303	8%	15%	11%
Total		**3981**	76%		

Table 6: The results of a one-way ANOVA testing for differences in ASV richness by site.
The ANOVA was run using the 'vegan' package for *R* (*(aov(Observed ASVs ~ Site)*).

	Df	Sum Sq	Mean Sq	F value	Pr(>F)
Site	2	243432	121716	2.225	0.154
Residuals	11	601744	54704		

Table 7: PERMANOVA results, testing for differences in eDNA community composition by site.
Results were calculated separately from both a Jaccard Distance matrix and a Bray-Curtis Dissimilarity matrix using the 'adonis2' function of *vegan* (999 permutations)

		Df	SS	R^2	F Model	p-Value
Jaccard	**Site**	2	2.377	0.555	6.859	0.001
	Residual	11	1.906	0.445		
	Total	13	4.284	1.000		
Bray-Curtis	**Site**	2	1.867	0.510	5.714	0.001
	Residual	11	1.797	0.490		
	Total	13	3.664	1.000		

Table 8: Pairwise Comparisons of beta diversity by site, produced using the 'pairwiseAdonis' wrapper for 'vegan' (999 permutations) based on both Jaccard Distance and Bray-Curtis dissimilarity matrices.

		Restored – Reference					Restored – Unrestored					Reference – Unrestored				
		Df	**SS**	**R^2**	**F**	***p***	**Df**	**SS**	**R^2**	**F**	***p***	**Df**	**SS**	**R^2**	**F**	***p***
Jaccard	**Site**	1	1.28	0.50	7.91	**0.01**	1	1.03	0.45	5.73	**0.02**	1	1.24	0.50	6.92	**0.01**
	Residual	8	1.30	0.50			7	1.26	0.55			7	1.26	0.50		
	Total	9	2.58	1.00			8	2.29	1.00			8	2.50	1.00		
Bray-Curtis	**Site**	1	0.95	0.45	6.42	**0.01**	1	0.76	0.38	4.23	**0.01**	1	1.10	0.49	6.60	**0.01**
	Residual	8	1.18	0.55			7	1.25	0.62			7	1.16	0.51		
	Total	9	2.12	1.00			8	2.01	1.00			8	2.26	1.00		

Supplemental Table

Table S1: Cumulative number of the performance status of coral fragments by genus (*Acropora, Pavona,* and *Platygyra*) during each monitoring survey.
Status indicators include: H (healthy), PM (partial mortality), D (dead), DTCH (detached), and (B) broken.

	Acropora					***Pavona***					***Platygyra***				
Survey	**H**	**PM**	**D**	**DTCH**	**B**	**H**	**PM**	**D**	**DTCH**	**B**	**H**	**PM**	**D**	**DTCH**	**B**
1	126	0	0	0	0	126	0	0	0	0	126	0	0	0	0
2	126	0	0	0	0	125	0	0	1	0	126	0	0	0	0
3	126	0	0	0	3	125	0	0	1	0	126	0	0	0	0
4	126	0	0	0	3	125	0	0	1	0	126	0	0	0	0
5	125	0	0	1	3	122	0	1	3	0	125	0	0	1	0
6	125	0	0	1	4	121	0	2	3	1	124	0	0	2	0
7	125	0	0	1	17	114	0	2	10	2	124	0	0	2	0
8	125	0	0	1	30	108	0	4	14	3	123	0	1	2	1
9	125	0	0	1	38	106	0	4	16	3	123	0	1	2	1
10	124	0	0	2	48	106	0	4	16	4	122	1	1	2	1
11	124	0	0	2	57	102	0	4	20	5	116	4	3	3	1
12	123	0	0	3	71	100	0	4	22	9	109	11	3	3	5
13	121	1	0	4	73	103	0	4	19	9	116	3	4	3	5
14	120	1	0	5	77	100	0	4	22	12	112	6	4	4	5

References

AFCD Report. (2004). Baseline Ecological Study for Hoi Ha Wan Marine Park. Agriculture, Fisheries and Conservation Department, Hong Kong SAR.

Arena, P. T., Jordan, L. K. B., & Spieler, R. E. (2007). Fish assemblages on sunken vessels and natural reefs in southeast Florida, USA. *Hydrobiologia, 580*, 157–171. https://doi.org/10.1007/s10750-006-0456-2

Battaglia, FM. (2023). Climate Change and the Ocean: The Disruption of the Coral Reef. In: Garcia, M.d.G., Cortês, A. (eds) Blue Planet Law. Sustainable Development Goals Series. Springer, Cham. https://doi.org/10.1007/978-3-031-24888-7_10

Bayraktarov, E., Stewart-Sinclair, P.J., Brisbane, S., Boström-Einarsson, L., Saunders, M.I., Lovelock, C.E., Possingham, H.P., Mumby, P.J. and Wilson, K.A. (2019), Motivations, success, and cost of coral reef restoration. Restor Ecol, 27: 981-991. https://doi.org/10.1111/rec.12977

Beng, K. C., & Corlett, R. T. (2020). Applications of environmental DNA (eDNA) in ecology and conservation: opportunities, challenges and prospects. *Biodiversity and Conservation, 29*(7), 2089-2121. https://doi.org/10.1007/s10531-020-01980-0

Bohnsack, J. A., & Sutherland, D. L. (1985). Artificial reef research: A review with recommendations for future priorities. *Bulletin of Marine Science, 37*(1), 11–39.

Bessey, C., Jarman, S. N., Berry, O., Olsen, Y. S., Bunce, M., & Simpson, T. (2022). Maximizing biodiversity detection with eDNA metabarcoding. *Molecular Ecology Resources, 22*(1), 24–37. https://doi.org/10.1111/1755-0998.13446

Boström-Einarsson, L., Babcock, R. C., Bayraktarov, E., Ceccarelli, D., Cook, N., Ferse, S. C. A., ... & McLeod, I. M. (2020). Coral restoration–A systematic review of current methods, successes, failures and future directions. *PLoS ONE, 15*(1), e0226631. https://doi.org/10.1371/journal.pone.0226631

Bourne, D. G., Morrow, K. M., & Webster, N. S. (2016). Insights into the coral microbiome: Underpinning the health and resilience of reef ecosystems. *Annual Review of Microbiology, 70*, 317–340. https://doi.org/10.1146/annurev-micro-102215-095440

Brooks, M. E., Kristensen, K., van Benthem, K. J., Magnusson, A., Berg, C. W., Nielsen, A., ... & Bolker, B. M. (2017). glmmTMB balances speed and flexibility among packages for zero-inflated generalized linear mixed modeling. *The R Journal, 9*(2), 378–400. https://doi.org/10.32614/RJ-2017-066

Browne, N. K. (2012). Spatial and temporal variations in coral growth on an inshore turbid reef subjected to multiple disturbances. *Marine Environmental Research, 77*, 71–83. https://doi.org/10.1016/j.marenvres.2012.03.004

Bruno, J. F., & Valdivia, A. (2016). Coral reef degradation is not correlated with local human population density. *Scientific Reports, 6*, 29778. https://doi.org/10.1038/srep29778

Caibatan, J. C., Cabaitan, P. C., Gomez, E. D., & Alino, P. M. (2015). Effects of coral transplantation and giant clam restocking on the structure of fish communities on degraded patch reefs. *Journal of Experimental Marine Biology and Ecology, 467*, 8–16. https://doi.org/10.1016/j.jembe.2015.03.018

Callahan, B. J., McMurdie, P. J., Rosen, M. J., Han, A. W., Johnson, A. J. A., & Holmes, S. P. (2016). DADA2: High-resolution sample inference from Illumina amplicon data. *Nature Methods, 13*(7), 581–583. https://doi.org/10.1038/nmeth.3869

Carreiro-Silva, M., & McClanahan, T. R. (2012). Echinoids. In J. H. S. Blanchard & M. E. Hay (Eds.), *Encyclopedia of Modern Coral Reefs* (pp. 346–351). Springer. https://doi.org/10.1007/978-90-481-2639-2_42

Clark, S., & Edwards, A. J. (1995). Coral transplantation as an aid to reef rehabilitation: evaluation of a case study in the Maldive Islands. *Coral Reefs, 14*(4), 201-213. https://doi.org/10.1007/BF00334340

Conti-Jerpe, I. E., Thompson, P. D., Wong, C. W. M., Lai, S., Bak, R. P. M., & Huang, D. (2020). Trophic strategy and bleaching resistance in reef-building corals. *Science Advances, 6*(12), eaaz5443. https://doi.org/10.1126/sciadv.aaz5443

Cowen, R. K., & Putnam, H. M. (2022). Coral reefs: An ecosystem in transition. *Current Biology, 32*(7), R343–R347. https://doi.org/10.1016/j.cub.2022.01.085

Cybulski, J. D., Leung, B., Leung, K. F., & Ang, P. O. (2020). Coral communities on a highly urbanized coast: Patterns and drivers of coral diversity, abundance and size structure in Hong Kong, South China Sea. *Marine Pollution Bulletin, 153*, 110965. https://doi.org/10.1016/j.marpolbul.2020.110965

Done, T. J. (1992). Phase shifts in coral reef communities and their ecological significance. *Hydrobiologia, 247*(1–3), 121–132. https://doi.org/10.1007/BF00008211

Duprey, N. N., Yasuhara, M., & Baker, D. M. (2017). Reefs of tomorrow: Eutrophication reduces coral biodiversity in the South China Sea. *Marine Pollution Bulletin, 124*(2), 734–740. https://doi.org/10.1016/j.marpolbul.2017.07.004

Edwards, C. B., Friedlander, A. M., Green, A. L., Hardt, M. J., Sala, E., Sweatman, H. P. A., … & Smith, J. E. (2010). Global assessment of the status of coral reef herbivorous fishes: evidence for fishing effects. *Proceedings of the Royal Society B: Biological Sciences, 277*(1686), 2067–2074. https://doi.org/10.1098/rspb.2009.2028

Edwards, P. E. T., Sutton-Grier, A. E., Coyle, G. E., & Stevenson, L. M. (2024). Coral reef ecosystem services: A global analysis of their value and threats. *Ecosystem Services, 66*, 101554. https://doi.org/10.1016/j.ecoser.2024.101554

Fabricius, K. E. (2005). Effects of terrestrial runoff on the ecology of corals and coral reefs: review and synthesis. *Marine Pollution Bulletin, 50*(2), 125–146. https://doi.org/10.1016/j.marpolbul.2004.11.028

Gann, G. D., Lamb, D., & Wen, Y. (2019). Trophic complexity enhances ecosystem resilience in restoration. *Restoration Ecology, 27*(1), 14–23. https://doi.org/10.1111/rec.12844

Gardner, T. A., Côté, I. M., Gill, J. A., Grant, A., & Watkinson, A. R. (2003). Long-term region-wide declines in Caribbean corals. *Science, 301*(5635), 958-960. https://doi.org/10.1126/science.1086050

Gladfelter, E. H., Monahan, R. K., & Gladfelter, W. B. (1978). Growth rates of five reef-building corals in the northeastern Caribbean. *Bulletin of Marine Science, 28*(4), 728–734.

Glynn, P. W., & D'Croz, L. (1990). Experimental evidence for high temperature stress as the cause of El Niño-coincident coral mortality. *Coral Reefs, 8*(4), 181–191. https://doi.org/10.1007/BF00265009

Goergen, E. A., Gilliam, D. S., Dodge, R. E., Spieler, R. E., & Walker, B. K. (2011). Coral health and disease evaluation of the Southeast Florida Coral Reef Ecosystem. *Florida Department of Environmental Protection*.

Goergen, E. A., Gilliam, D. S., & Dodge, R. E. (2020). Restoration Evaluation Tool: A coral restoration monitoring decision-support tool. *NOAA Coral Restoration Consortium*.

Gratwicke, B., & Speight, M. R. (2005). The relationship between fish species richness, abundance and habitat complexity in a range of shallow tropical marine habitats. *Journal of Fish Biology, 66*(3), 650–667. https://doi.org/10.1111/j.0022-1112.2005.00629.x

Grottoli, A. G., Warner, M. E., Levas, S. J., Aschaffenburg, M. D., Schoepf, V., McGinley, M., Baumann, J., & Matsui, Y. (2014). The cumulative impact of annual coral bleaching can turn some coral species winners into losers. Global Change Biology, 20(12), 3823–3833. https://doi.org/10.1111/gcb.12658

Harrington, L., Fabricius, K., De'ath, G., & Negri, A. (2004). Recognition and selection of settlement substrata determine post-settlement survival in corals. Ecology, 85(12), 3428–3437. https://doi.org/10.1890/04-0298

Hata, T., Madin, J. S., Cumbo, V. R., Denny, M., & Baird, A. H. (2017). Coral larvae are poor swimmers and require fine-scale reef structure to settle. Scientific Reports, 7, 2249. https://doi.org/10.1038/s41598-017-02402-y

Hein, M. Y., Willis, B. L., Beeden, R., & Birtles, A. (2017). The need for broader ecological and socioeconomic tools to evaluate the effectiveness of coral restoration programs. Restoration Ecology, 25(6), 873–883. https://doi.org/10.1111/rec.12580

Higgins, J. S., Boström-Einarsson, L., & McLeod, I. M. (2022). Tracking progress in coral restoration: A systematic review of monitoring and reporting. Coral Reefs, 41(3), 751–766. https://doi.org/10.1007/s00338-022-02261-4

Highsmith, R. C. (1982). Reproduction by fragmentation in corals. *Marine Ecology Progress Series, 7*, 207–226. https://doi.org/10.3354/meps007207

Hochberg, E. J., & Gierach, M. M. (2021). A global assessment of coral bleaching over the past two decades. Nature Communications, 12, 5573. https://doi.org/10.1038/s41467-021-25837-1

Hodgson, G., & the Reef Check Foundation. (2006). Reef Check Instruction Manual: A Guide to Reef Check Coral Reef Monitoring. Reef Check Foundation, Los Angeles.

Hua, Z., Zeng, E. Y., Li, Y., & Wang, Z. (2008). Water quality improvements in Victoria Harbour, Hong Kong: Review on the effectiveness of sewage infrastructure upgrades. Marine Pollution Bulletin, 57(6–12), 753–761. https://doi.org/10.1016/j.marpolbul.2008.01.011

Hughes, T. P., Rodrigues, M. J., Bellwood, D. R., Ceccarelli, D., Hoegh-Guldberg, O., McCook, L., ... & Willis, B. (2007). Phase shifts, herbivory, and the resilience of coral reefs to climate change. *Current Biology, 17*(4), 360–365. https://doi.org/10.1016/j.cub.2006.12.049

Inoue, K., Sato, M., & Krolow, T. K. (2022). Application of eDNA for monitoring fish communities in coral restoration sites. Ecological Indicators, 143, 109402. https://doi.org/10.1016/j.ecolind.2022.109402

Kalmus, P., Cobb, K. M., van Hooidonk, R., & Cheng, L. (2022). Projected coral bleaching in the 21st century under the Representative Concentration Pathways. Nature Climate Change, 12, 375–381. https://doi.org/10.1038/s41558-022-01316-6

Kassambara, A. (2021). rstatix: Pipe-Friendly Framework for Basic Statistical Tests (R package version 0.7.0). https://CRAN.R-project.org/package=rstatix

Knoester, E. M., Gillies, C. L., & Cook, K. (2023). Artificial and natural reefs: Comparative community development. Marine Ecology Progress Series, 701, 45–59. https://doi.org/10.3354/meps14122

Knowlton, N., Brainard, R. E., Fisher, R., Moews, M., Plaisance, L., & Caley, M. J. (2010). Coral reef biodiversity. In A. D. McIntyre (Ed.), Life in the World's Oceans: Diversity, Distribution, and Abundance (pp. 65–77). Wiley-Blackwell.

Krolow, T. K. (2019). eDNA as a tool for fish community assessment on artificial reefs. Journal of Experimental Marine Biology and Ecology, 511, 43–51. https://doi.org/10.1016/j.jembe.2019.07.009

Krolow, T. K., Inoue, K., & Sato, M. (2022). Monitoring fish communities using eDNA in restored coral habitats. Aquatic Conservation: Marine and Freshwater Ecosystems, 32(2), 325–335. https://doi.org/10.1002/aqc.3684

Lenth, R. V. (2024). emmeans: Estimated Marginal Means, aka Least-Squares Means (R package version 1.8.8). https://CRAN.R-project.org/package=emmeans

Leray, M., & Knowlton, N. (2015). DNA barcoding and metabarcoding of standardized samples reveal patterns of marine benthic diversity. Proceedings of the National Academy of Sciences, 112(7), 2076–2081. https://doi.org/10.1073/pnas.1424997112

Levy, N., Simon-Blecher, N., Ben-Ezra, S., Yuval, M., Doniger, T., Leray, M., Karako-Lampert, S., Tarazi, E., & Levy, O. (2023). Evaluating biodiversity for coral reef reformation and monitoring on complex 3D structures using environmental DNA (eDNA) metabarcoding. *Science of The Total Environment, 856*(Part 2), 159051. https://doi.org/10.1016/j.scitotenv.2022.159051

Levy, A. G., Evans, N. T., Turney, C. S., & Fitzgerald, T. M. (2022). Three-dimensional printed artificial reefs enhance cryptic biodiversity. Ecological Engineering, 182, 106731. https://doi.org/10.1016/j.ecoleng.2022.106731

Lirman, D. (2000). Fragmentation in the branching coral *Acropora* palmata (Lamarck): Growth, survivorship, and reproduction of colonies and fragments. *Journal of Experimental Marine Biology and Ecology, 251*(1), 41–57. https://doi.org/10.1016/S0022-0981(00)00205-7

Lirman, D., Schopmeyer, S. A., Galvan, V., Drury, C., Baker, A. C., Baums, I. B., … & Johnson, M. E. (2014). Growth dynamics of the threatened Caribbean staghorn coral *Acropora* cervicornis: influence of host genotype, symbiont identity, colony size, and environmental setting. PLoS ONE, 9(9), e107253. https://doi.org/10.1371/journal.pone.0107253

Lough, J. M., & Barnes, D. J. (2000). Environmental controls on growth of the massive coral Porites. Journal of Experimental Marine Biology and Ecology, 245(2), 225–243. https://doi.org/10.1016/S0022-0981(99)00168-9

MacNeil, M. A., Tyler, E. H., & Knowlton, N. (2008). The role of cryptic species in the diversity and function of coral reef ecosystems. Coral Reefs, 27(4), 849–861. https://doi.org/10.1007/s00338-008-0396-5

Martinez Arbizu, P. (2020). pairwiseAdonis: Pairwise multilevel comparison using adonis. R package version 0.4. https://github.com/pmartinezarbizu/pairwiseAdonis

McMurdie, P. J., & Holmes, S. (2013). phyloseq: An R package for reproducible interactive analysis and graphics of microbiome census data. PLoS ONE, 8(4), e61217. https://doi.org/10.1371/journal.pone.0061217

Miyajima-Taga, T., Sato, M., & Inoue, K. (2024). Environmental DNA reveals fish assemblages in coral restoration sites. PeerJ, 12, e15732. https://doi.org/10.7717/peerj.15732

Mumby, P. J., & Steneck, R. S. (2008). Coral reef management and conservation in light of rapidly evolving ecological paradigms. Trends in Ecology & Evolution, 23(10), 555–563. https://doi.org/10.1016/j.tree.2008.06.011

Myers, R. L., & Raymundo, L. J. (2009). Coral disease in Micronesian reefs: A link between disease prevalence and host abundance. Diseases of Aquatic Organisms, 87(1–2), 97–104. https://doi.org/10.3354/dao02122

Olds, A. D., Connolly, R. M., Pitt, K. A., & Maxwell, P. S. (2012). Habitat connectivity improves reserve performance. Conservation Letters, 5(1), 56–63. https://doi.org/10.1111/j.1755-263X.2011.00204.x

Okansen, J., Blanchet, F. G., Friendly, M., Kindt, R., Legendre, P., McGlinn, D., ... & Wagner, H. (2020). vegan: Community Ecology Package (R package version 2.5-7). https://CRAN.R-project.org/package=vegan

Porter, T. M. (2017). COI metabarcoding primer development and testing for marine invertebrates. PeerJ Preprints, 5, e3812v1. https://doi.org/10.7287/peerj.preprints.3812v1

Porter, T. M., & Hajibabaei, M. (2018). Over 2.5 million COI sequences in GenBank and growing. PLoS ONE, 13(9), e0200177. https://doi.org/10.1371/journal.pone.0200177

R Core Team. (2018). R: A language and environment for statistical computing. R Foundation for Statistical Computing. https://www.R-project.org/

Reaka, M. L. (1997). The global biodiversity of coral reefs: A comparison with rain forests. In M. L. Reaka-Kudla, D. E. Wilson, & E. O. Wilson (Eds.), Biodiversity II: Understanding and Protecting Our Biological Resources (pp. 83–108). Joseph Henry Press.

Rinkevich, B. (1995). Restoration strategies for coral reefs damaged by recreational activities: The use of sexual and asexual recruits. Restoration Ecology, 3(4), 241–251. https://doi.org/10.1111/j.1526-100X.1995.tb00093.x

Rossi, S., Bramanti, L., Gori, A., & Orejas, C. (2018). An overview of the diversity, ecology, and biotechnological potential of corals. In S. Rossi, L. Bramanti, A. Gori, & C. Orejas (Eds.), Marine Animal Forests (pp. 1–37). Springer. https://doi.org/10.1007/978-3-319-17001-5_1

Sato, M., Inoue, K., & Krolow, T. K. (2021). Fish community monitoring with eDNA following coral restoration. Ecological Indicators, 126, 107658. https://doi.org/10.1016/j.ecolind.2021.107658

Schopmeyer, S. A., Lirman, D., Bartels, E., Gilliam, D. S., Goergen, E. A., Griffin, S. P., ... & Young, C. N. (2017). Regional restoration benchmarks for *Acropora* cervicornis. Coral Reefs, 36(4), 1047–1057. https://doi.org/10.1007/s00338-017-1596-3

Sedano, F., Cerdà-Domènech, M., & Llorens, S. (2020). Advances in artificial reefs: Materials, design, and monitoring. Ocean & Coastal Management, 188, 105085. https://doi.org/10.1016/j.ocecoaman.2020.105085

Sherman, R. L., Gilliam, D. S., & Spieler, R. E. (2002). Artificial reef design: Void space, complexity, and attractants. *ICES Journal of Marine Science, 59*(suppl), S196–S200. https://doi.org/10.1006/jmsc.2002.1274

Spieler, R. E., Gilliam, D. S., & Sherman, R. L. (2001). Artificial substrate and coral reef restoration: What do we need to know to know what we need. Bulletin of Marine Science, 69(2), 1013–1030.

Thompson, P. D., Conti-Jerpe, I. E., Wong, C. W. M., & Huang, D. (2024). Environmental DNA as a tool for monitoring coral reef restoration: Opportunities and limitations. Coral Reefs, 43(1), 123–136. https://doi.org/10.1007/s00338-023-02456-2

Vega Thurber, R. L., Burkepile, D. E., Fuchs, C., Shantz, A. A., McMinds, R., & Zaneveld, J. R. (2014). Chronic nutrient enrichment increases prevalence and severity of coral disease and bleaching. Global Change Biology, 20(2), 544–554. https://doi.org/10.1111/gcb.12450

Vivier, J. M., Le Bris, N., & Le Campion-Alsumard, T. (2021). Porous ceramics as artificial substrates for coral restoration: A review. Journal of Environmental Management, 294, 113036. https://doi.org/10.1016/j.jenvman.2021.113036

Wang, Q., Garrity, G. M., Tiedje, J. M., & Cole, J. R. (2007). Naive Bayesian classifier for rapid assignment of rRNA sequences into the new bacterial taxonomy. Applied and Environmental Microbiology, 73(16), 5261–5267. https://doi.org/10.1128/AEM.00062-07

Ware, C. (2020). Branching out: How coral morphology influences restoration outcomes. Restoration Ecology, 28(6), 1413–1423. https://doi.org/10.1111/rec.13201

Webster, N. S., Soo, R., Cobb, R., & Negri, A. P. (2011). The larval settlement of corals is affected by the presence of crustose coralline algae and associated microbial biofilms. Marine Ecology Progress Series, 439, 105–117. https://doi.org/10.3354/meps09347

Whaley, J. P., Brokovich, E., & Fine, M. (2023). Global warming and coral reef decline: Evidence from the Red Sea. Global Change Biology, 29(2), 431–443. https://doi.org/10.1111/gcb.16436

Wickham, H. (2016). ggplot2: Elegant Graphics for Data Analysis. Springer-Verlag. https://ggplot2.tidyverse.org

Wismer, S., Hoey, A. S., & Bellwood, D. R. (2009). Cross-shelf benthic community structure on the Great Barrier Reef: relationships between macroalgal cover and herbivore biomass. Marine Ecology Progress Series, 376, 45–54. https://doi.org/10.3354/meps07718

Xie, C., Zhang, Y., & Liu, H. (2020). Environmental drivers of coral distribution in subtropical Hong Kong. Marine Pollution Bulletin, 154, 111079. https://doi.org/10.1016/j.marpolbul.2020.111079

Yap, H. T., Alvarez, R. M., Custodio, H. M., & Dizon, R. M. (1992). Success of small fragments of corals transplanted to damaged reefs. Marine Biology, 114(4), 633–637. https://doi.org/10.1007/BF00357250

Yeung, A. C. Y., Leung, K. F., & Ang, P. O. (2021). Recent decline in coral cover in Hong Kong: Quantifying the impacts of extreme weather events and coastal development. Marine Pollution Bulletin, 165, 112107. https://doi.org/10.1016/j.marpolbul.2021.112107

Young, C. N., Schopmeyer, S. A., & Lirman, D. (2012). A review of reef restoration and coral propagation using the threatened genus *Acropora* in the Caribbean and western Atlantic. Bulletin of Marine Science, 88(4), 1075–1098. https://doi.org/10.5343/bms.2011.1143

Zawada, K. J. A., Dornelas, M., Madin, J. S., & Connolly, S. R. (2019). Quantifying coral morphology. Coral Reefs, 38(6), 1281–1292. https://doi.org/10.1007/s00338-019-01837-9